Wiley
Complexity
Volume 2024, Article ID 6878662, 36 pages
https://doi.org/10.1155/2024/6878662

WILEY

Research Article

Modeling the Effects of *Ehrlichia chaffeensis* and Movement on Dogs

Folashade B. Agusto and Jaimie Drum

Department of Ecology and Evolutionary Biology, University of Kansas, Lawrence, KS, USA

Correspondence should be addressed to Folashade B. Agusto; fbagusto@gmail.com

Received 9 January 2024; Revised 13 April 2024; Accepted 7 May 2024

Academic Editor: Ning Cai

Ehrlichia chaffeensis is a tick-borne infectious disease transmitted by *Amblyomma americanum* tick. This infectious disease was discovered in the 1970s when military dogs were returning from the Vietnam War. The disease was found to be extremely severe in German Shepherds, Doberman Pinschers, Belgium Malinois, and Siberian Huskies. In this study, we developed a mathematical model for dogs and ticks infected with *Ehrlichia chaffeensis* with the aim of understanding the impact of movement on dogs as they move from one location to another. This could be a dog taken on a walk in an urban area or on a hike in the mountains. We carried out a global sensitivity analysis with and without movement between three locations using as response functions the sum of acutely and chronically infected ticks and the sum of infected ticks in all life stages. The parameters with the most significant impact on the response functions are dogs disease progression rate, dogs chronic infection progression rate, dogs recovery rate, dogs natural death rate, acutely and chronically infected dogs disease-induced death rate, dogs birth rate, eggs maturation rates, tick biting rate, dogs and ticks transmission probabilities, ticks death rate, and the location carrying capacity. Our simulation results show that infection in dogs and ticks are localized in the absence of movement and spreads between locations with highest infection in locations with the highest rate movement. Also, the effect of the control measures which reduces infection trickles to other locations (trickling effect) when controls are implemented in a single location. The trickling effect is strongest when control is implemented in a location with the highest movement rate into it.

1. Introduction

Ehrlichia chaffeensis is a tick-borne infectious disease that lives within white blood cells. The disease was first recognized in Africa during the 1930s. This infectious disease originated in the United States in the 1970s, when military dogs were returning from the Vietnam War. It is estimated that 200–250 million dogs died from this disease in Vietnam. Due to the high infection rates of dogs a majority of the war dogs were left behind in Vietnam [1]. They found this disease to be extremely severe in German Shepherds, Doberman Pinschers, Belgium Malinois, and Siberian Huskies. This disease can also be referred to as tracker dog disease and tropical canine pancytopenia [2].

One primary vector of *Ehrlichia chaffeensis* is the *Amblyomma americanum* tick. It is mostly found in south-central and eastern United States [3]. It is also referred to as the Lone Star tick. The tick goes through four different life stages. These life stages are egg, larvae, nymph, and adult, which typically take two years to complete [4]. The adult ticks are typically the ones that feed on dogs. They are seen active March through August in the Midwest [5]. There is currently no vaccine for dogs in preventing *Ehrlichia Chaffeensis*. The way of prevention is by preventing ticks on pets and in yards.

There are two stages of infection with *Ehrlichia chaffeensis* in dogs. The first 2–4 weeks of infection are referred to as the acute stage. During this stage, symptoms include fever, swollen lymph nodes, respiratory distress, weight loss, bleeding disorders, and sometimes neurological disturbances. There is an antibody and PCR test for *Ehrlichia chaffeensis* in dogs. The antibody test could remain negative

during the first week of illness and could remain positive for months to years. There is a rapid antibody test that gives results within minutes or there is an ELISA and IFA antibody test that takes days or weeks for results. The PCR test can provides species-specific results and can take days for results. Dogs are treated for *Ehrlichia chaffeensis* with a 28-day treatment of doxycycline. After 24–72 hours of initiating treatment the clinical signs should resolve [6]. After 2–4 weeks the dog will recover or progress into the clinical/chronic stage. During the clinical/chronic stage dogs may develop symptoms such as anemia, bleeding episodes, lameness, eye problems, neurological problems, and swollen limbs. The clinical/chronic stage typically leads to death [2]. There is no correlation between the age of dog and the severity of the infection stage [7]. Dogs are capable of being reinfected of *Ehrlichia chaffeensis*; however, dogs cannot pass the disease on to their offspring.

To prevent dogs from being infected with *Ehrlichia chaffeensis,* it is advised to use proper tick prevention techniques. This may include collars, monthly topical, or oral preventatives year round. It is not recommended to use human insect repellent on dogs. After dogs have spent time outside it is recommended to thoroughly evaluate them for ticks. Removing a tick right away reduces the risk of disease transmission. To remove a tick, it is recommended to use fine-tipped tweezers and grab the tick closely to the skin's surface. Then proceed to pull with a steady pressure upwards [6].

The goal of this study is to produce a mathematical model to better understand the transmission of *Ehrlichia chaffeensis* between dogs and *Amblyomma americanum*. This model will also be used to better understand the impact of movement on dogs as they move from one location to another. This could be taking a dog on a walk in an urban area or taking a dog on a hike in the mountains. A preprint of this study is already available on bioRxiv [8].

The rest of the paper is organized as follows: in Section 2, we present the *Ehrlichia chaffeensis* mathematical model for a single location with no movement, the basic qualitative analysis of the model including results of the positivity and boundedness of solutions, the computation of the reproduction number, and global sensitivity analysis. In Section 3, we introduce the *Ehrlichia chaffeensis* model with movement between different locations. In this section, we also implement a global sensitivity analysis in the absence and presence of movement. Using results from the sensitivity analysis we simulate the model with movement to determine the effect of disease transmission and ticks natural death when the locations are isolated and when they are connected by movement. In Section 4, we discuss and give conclusions of the results obtained from this study, followed by some recommendations to dog owners.

2. Model Formulation

We formulate the transmission model of *Ehrlichia chaffeensis* by incorporating two subgroups: dogs and ticks, and follow the approach in [9]. The dog population is divided into susceptible (S_D), exposed (E_D), acute infection (A_D), chronic infection (C_D), and recovered (R_D). Therefore, the total population of dogs is given by

$$N_D = S_D + E_D + A_D + C_D + R_D. \tag{1}$$

The tick population was divided into egg, larvae, nymph, and adult ticks classes. Each of these contained a susceptible class (S_{Ti}) and infections class (I_{Ti}), where $i = E, L, N$, and A, for egg, larvae, nymph and adult classes. As previously mentioned *Ehrlichia chaffeensis* is not transmitted to offspring, so the tick eggs do not have an infection class. Therefore, the total tick population is defined as

$$N_T = S_{TL} + I_{TL} + S_{TN} + I_{TN} + S_{TA} + I_{TA}. \tag{2}$$

The susceptible dog (S_D) compartment is increased due to an increase in newborn dogs. The susceptible (S_D) dogs compartment decreases due to a natural death rate (μ_D). The force of infection in dogs is represented as

$$\lambda_D = \frac{\beta_D \phi_T \left(I_{TL} + I_{TN} + I_{TA}\right)}{N_D}, \tag{3}$$

where the parameter β_D is the probability of dog transmission. The parameter ϕ_T represents the rate at which a tick bites a dog. It is assumed that the ticks are all biting at a constant rate. The susceptible dogs progress out of the susceptible compartment at a rate (λ_D) to the exposed compartment. The equation for the susceptible dog population compartment is given as

$$\frac{dS_D}{dt} = \theta_D - \lambda_D S_D - \mu_D S_D. \tag{4}$$

The population of exposed dogs increases at a rates $f\lambda_D$ and $\varepsilon\lambda_D$. These rates come from infected susceptible dogs and the reinfection of dogs that have recovered from *Ehrlichia chaffeensis*. It is found that dogs can only recover from the acute stage of infection since chronic stage illnesses lead to death [10]. Population this compartment decreases due to natural death rate (μ_D) and disease progression at the rate (σ_D). The exposed dogs compartment is represented by the following equation:

$$\frac{dE_D}{dt} = \lambda_D S_D + \varepsilon\lambda_D R_D - \sigma_D E_D - \mu_D E_D. \tag{5}$$

The acute stage compartment (A_D) increases from the exposed dog compartment and decreases at a natural death rate of μ_D and an infectious death rate of δ_D. It can also decrease at a recovery rate of γ_D or at a progression of infection into the chronic stage at a rate of υ_D. The acute stage of the infection in dogs (A_D) can be represented as

$$\frac{dA_D}{dt} = \sigma_D E_D - \nu_D A_D - \gamma_D A_D - \mu_D A_D - \delta_D A_D. \tag{6}$$

The population of dogs in the chronic stage compartment (C_D) increases from the acute stage compartment. This compartment can only decrease due to natural death (μ_D) or disease induced death at the rate δ_D. The chronic stage of this illness can be managed in dogs, however, it eventually will lead to death, therefore, it does not lead to the

recovery of the dogs [10]. The chronic stage (C_D) is represented by the following equation:

$$\frac{dC_D}{dt} = \nu_D A_A - \mu_D C_A - \delta_D C_A. \tag{7}$$

The last compartment of the dog model is the recovered stage (R_D). This compartment increases from the acute stage of the disease. At the recovered stage the dog is no longer infectious; therefore, it doesn't contain an infection death rate. It decreases due to natural death rate (μ_D) or due to a reinfection in the dog ($\varepsilon\lambda_D$). The recovered stage compartment (R_D) is represented as

$$\frac{dR_D}{dt} = \gamma_D A_A - \varepsilon\lambda_D R_D - \mu_D R_D. \tag{8}$$

Amblyomma americanum ticks transmit *Ehrlichia chaffeensis* transstadially (eggs to larvae to nymph to adults) but not transovarially (adults to eggs) [11]. The susceptible ticks move to infectious tick at a rate λ_T which is represented as

$$\lambda_T = \frac{\beta_T \phi_T \left(E_D + A_D + C_D\right)}{N_D}, \tag{9}$$

where the parameter β_T represents the probability of tick transmission. The parameter ϕ_T represents the rate at which the ticks bite. The susceptible and infection tick larvae have a maturation rate of σ_L and a natural death rate of μ_L. These equations are represented as

$$\begin{aligned} \frac{dS_{TL}}{dt} &= \alpha_E S_{TE} - \lambda_T S_{TL} - \alpha_L S_{TL} - \mu_L S_{TL}, \\ \frac{dI_{TL}}{dt} &= \lambda_T S_{TL} - \alpha_L I_{TL} - \mu_L I_{TL}. \end{aligned} \tag{10}$$

The maturation rate from nymphs to adults is α_N and a natural death rate of μ_N. These equations are represented as

$$\begin{aligned} \frac{dS_{TN}}{dt} &= \alpha_L S_{TL} - \lambda_T S_{TN} - \alpha_N S_{TN} - \mu_N S_{TN}, \\ \frac{dI_{TN}}{dt} &= \alpha_L I_{TL} + \lambda_T S_{TN} - \alpha_N I_{TN} - \mu_N I_{TN}. \end{aligned} \tag{11}$$

The susceptible and infected adult ticks (S_{TA} and I_{TA}) lay eggs at a rate of θ_A which is limited by the carrying capacity K. Therefore, the susceptible tick eggs and susceptible tick adults are represented as

$$\begin{aligned} \frac{dS_{TE}}{dt} &= \theta_A\left(1 - \frac{S_{TE}}{K}\right)\left(S_{TA} + I_{TA}\right) - \sigma_E S_{TE} - \mu_E S_{TE}, \\ \frac{dS_{TA}}{dt} &= \alpha_N S_{TN} - \lambda_T S_{TA} - \mu_A S_{TA}. \end{aligned} \tag{12}$$

Lastly, infected adults tick (I_{TA}) can only decrease at a death rate of μ_A. This is represented as

$$\frac{dI_{TA}}{dt} = \alpha_N I_{TN} + \lambda_T S_{TA} - \mu_A I_{TA}. \tag{13}$$

Given the assumptions above, the following nonlinear equations are given for the transmission of *Ehrlichia chaffeensis*:

$$\begin{aligned} \frac{dS_D}{dt} &= \theta_D - \lambda_D S_D - \mu_D S_D \\ \frac{dE_D}{dt} &= \lambda_D S_D + \varepsilon\lambda_D R_D - \sigma_D E_D - \mu_D E_D \\ \frac{dA_D}{dt} &= \sigma_D E_D - \nu_D A_D - \gamma_D A_D - \mu_D A_D - \delta_D A_D \\ \frac{dC_D}{dt} &= \nu_D A_D - \mu_D C_D - \delta_D C_D \\ \frac{dR_D}{dt} &= \gamma_D A_D - \varepsilon\lambda_D R_D - \mu_D R_D \\ \frac{dS_{TE}}{dt} &= \theta_A\left(1 - \frac{S_{TE}}{K}\right)\left(S_{TA} + I_{TA}\right) - \alpha_E S_{TE} - \mu_E S_{TE} \\ \frac{dS_{TL}}{dt} &= \alpha_E S_{TE} - \lambda_T S_{TL} - \alpha_L S_{TL} - \mu_L S_{TL} \\ \frac{dI_{TL}}{dt} &= \lambda_T S_{TL} - \alpha_L I_{TL} - \mu_L I_{TL} \\ \frac{dS_{TN}}{dt} &= \alpha_L S_{TL} - \lambda_T S_{TN} - \alpha_N S_{TN} - \mu_N S_{TN} \\ \frac{dI_{TN}}{dt} &= \alpha_L I_{TL} + \lambda_T S_{TN} - \alpha_N I_{TN} - \mu_N I_{TN} \\ \frac{dS_{TA}}{dt} &= \alpha_N S_{TN} - \lambda_T S_{TA} - \mu_A S_{TA} \\ \frac{dI_{TA}}{dt} &= \alpha_N I_{TN} + \lambda_T S_{TA} - \mu_A I_{TA}, \end{aligned} \tag{14}$$

where

$$\begin{aligned} \lambda_D &= \frac{\beta_D \phi_T \left(I_{TL} + I_{TN} + I_{TA}\right)}{N_D}, \\ \lambda_T &= \frac{\beta_T \phi_T \left(E_D + A_D + C_D\right)}{N_D}, \end{aligned} \tag{15}$$

and $N_D = S_D + E_D + A_D + C_D + R_D$.

The conceptualized flow diagram of the *Ehrlichia chaffeensis* transmission in dogs model is shown in Figure 1. The corresponding parameters and variables are described in Table 1.

2.1. Analysis of the Model

2.1.1. Basic Qualitative Properties

(1) Positivity and Boundedness of Solutions. For the *Ehrlichia chaffeensis* model (6) to be epidemiologically meaningful, it is important to prove that all its state variables are

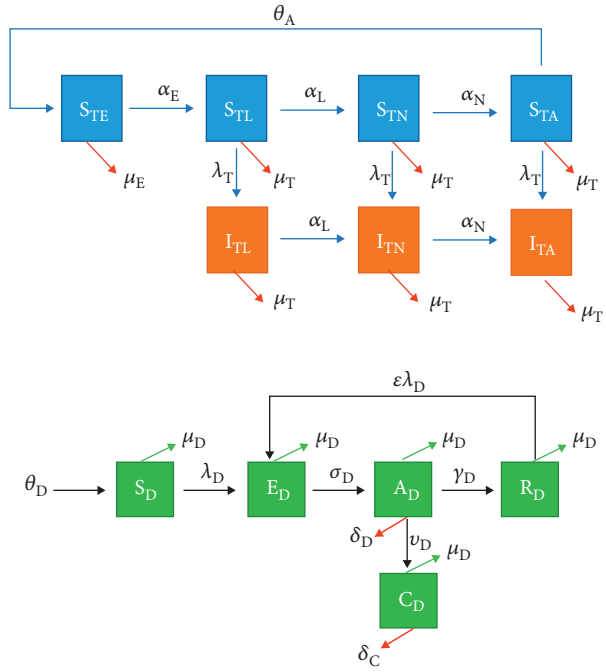

Figure 1: Flow diagram of *Ehrlichia chaffeensis* model (6). The dogs are divided into susceptible (S_D), exposed (E_D), acute infection (A_A), chronic infection (C_D), and recovered (R_D). The tick population is composed of susceptible (S_{Ti}) and infectious classes (I_{Ti}), where $i = E, L, N, A$ corresponding to egg, larvae, nymph, and adult ticks. The blue compartment represents susceptible ticks and the orange compartment represents infected ticks.

non-negative for all time. In other words, solutions of the model system (6) with non-negative initial data will remain non-negative for all time $t > 0$.

Lemma 1. *Let the initial data* $(0) \geq 0$, *where* $F(t) = (S_D(t), E_D(t), A_D(t), C_D(t), R_D(t), S_{TE}(t), S_{TL}(t), I_{TL}(t), S_{TN}(t), I_{TN}(t), S_{TA}(t), I_{TA}(t))$. *Then, the solutions* $F(t)$ *of the Ehrlichia chaffeensis model (6) are non-negative for all* $t > 0$. *Furthermore,*

$$\begin{aligned} \limsup_{t\longrightarrow\infty} N_D(t) &\leq \frac{\theta_D}{\mu_D}, \\ \limsup_{t\longrightarrow\infty} N_T(t) &\leq \frac{\theta_A K}{\mu_T}, \end{aligned} \tag{16}$$

where

$$N_D(t) = S_D(t) + E_D(t) + A_D(t) + C_D(t) + R_D(t), \tag{17}$$

Table 1: Description of the parameters and variables for the *Ehrlichia chaffeensis* model (6).

Variable	Description
S_D	Population of susceptible dogs
E_D	Population of exposed dogs
A_D	Population of acute stage of infection in dogs
C_D	Population of chronic stage of infection in dogs
R_D	Population of recovered dogs
S_{TE}	Susceptible tick eggs
S_{TL}, S_{TN}, S_{TA}	Population of susceptible larvae, nymphs, and adult ticks
I_{TE}	Infected tick eggs
I_{TL}, I_{TN}, I_{TA}	Population of infected larvae, nymphs, and adult ticks
Parameter	**Description**
θ_D	Birth rate of dogs
γ_D	Recovery rate in dogs
υ_D	Acute to chronic disease progression rate in dogs
σ_D	Disease progression rate in dogs
ε	Reinfection rate of in dogs
α_E	Tick eggs to larvae maturation rate
α_L	Larvae to nymphs maturation rate
α_N	Nymphs to adult ticks maturation rate
θ_A	Ticks egg laying rate
μ_E	Tick eggs decay rate
μ_L, μ_N, μ_A	Larvae, nymphs, adult ticks death rate
μ_D	Natural death rate of dogs
δ_D	Acute infection death rate in dogs
δ_C	Chronic infection death rate in dogs
β_D	Dog transmission probability
ϕ_T	Tick biting rate
β_T	Tick transmission probability

and

$$\begin{aligned} N_T(t) = {} & S_{TL}(t) + I_{TL}(t) + S_{TN}(t) \\ & + I_{TN}(t) + S_{TA}(t) + I_{TA}(t). \end{aligned} \tag{18}$$

The proof of Lemma 1 is given in Appendix A.

(2) Invariant Regions. The *Ehrlichia chaffeensis* model (14) will be analyzed in a biologically-feasible region as follows. Consider the feasible region

$$\Omega = \Omega_D \cup \Omega_T \subset \mathbb{R}_+^5 \times \mathbb{R}_+^7, \tag{19}$$

with,

$$\Omega_D = \left\{ (S_D(t), E_D(t), A_D(t), C_D(t), R_D(t)) \in \mathbb{R}_+^5 : N_D(t) \leq \frac{\theta_D}{\mu_D} \right\}, \tag{20}$$

and

$$\Omega_T = \left\{ \left(S_{TE}(t), S_{TL}(t), I_{TL}(t), S_{TN}(t), I_{TN}(t), S_{TA}(t), I_{TA}(t)\right) \in \mathbb{R}_+^7 \colon S_{TE}(t) \le K, N_T(t) \le \frac{\sigma_E K}{\mu_T} \right\}. \tag{21}$$

Lemma 2. *The region $\Omega = \Omega_D \cup \Omega_D \subset \mathbb{R}_+^5 \times \mathbb{R}_+^7$ is positively-invariant for the model (6) with non-negative initial conditions in $\mathbb{R}_+^{12}$.*

The prove of Lemma 2 is given in Appendix B.

In the next section, the conditions for the existence and stability of the equilibria of the model (6) are stated.

(3) Stability of Disease-Free Equilibrium (DFE). The *Ehrlichia chaffeensis* model has a disease-free equilibrium (DFE) denoted by $\mathscr{E}_0$. The DFE is obtained by setting the right-hand sides of the equations in the model (6) to zero, which is given by

$$\mathscr{E}_0 = (S_D^*, E_D^*, A_D^*, C_D^*, R_D^*, S_{TE}^*, S_{TL}^*, I_{TL}^*, S_{TN}^*, I_{TN}^*, S_{TA}^*, I_{TA}^*), \tag{22}$$

where

$$\begin{aligned} S_D^* &= \frac{\theta_D}{\mu_D}, \\ S_{TE}^* &= \frac{K\left(\alpha_E\alpha_L\alpha_N\theta_A - g_4g_5g_7\mu_T\right)}{\alpha_E\alpha_L\alpha_N\theta_A}, \\ S_{TL}^* &= \frac{K\left(\alpha_E\alpha_L\alpha_N\theta_A - g_4g_5g_7\mu_T\right)}{\alpha_L\alpha_N\theta_A g_5}, \\ S_{TN}^* &= \frac{K\left(\alpha_E\alpha_L\alpha_N\theta_A - g_4g_5g_7\mu_T\right)}{\alpha_N\theta_A g_5 g_7}, \\ S_{TA}^* &= \frac{K\left(\alpha_E\alpha_L\alpha_N\theta_A - g_4g5g_7\mu_T\right)}{\theta_A\mu_T g_2 g_4}, \end{aligned} \tag{23}$$

with $g_1 = \sigma_D + \mu_D, g_2 = \upsilon_D + \gamma_D + \mu_D + \delta_D, g_3 = \mu_D + \delta_C, g_4 = \sigma_E + \mu_E, g_5 = \alpha_L + \mu_T, g_6 = \alpha_L + \mu_T, g_7 = \alpha_N + \mu_T, g_8 = \alpha_N + \mu_T$, and $\mu_T = \min\{\mu_L, \mu_N, \mu_A\}$, and all other disease states are set equal to zero.

The stability of $\mathscr{E}_0$ can be established using the next generation operator method on system (6). Taking $E_D, A_D, C_D, I_{TL}, I_{TN}$, and I_{TA} as the infected compartments and then using the notation in [12], the Jacobian F and V matrices for new infectious terms and the remaining transfer terms, respectively, are defined as

$$F = \begin{pmatrix} 0 & 0 & 0 & \beta_D\phi_T & \beta_D\phi_T & \beta_D\phi_T \\ 0 & 0 & 0 & 0 & 0 & 0 \\ 0 & 0 & 0 & 0 & 0 & 0 \\ \frac{\beta_T\phi_T S_{TL}^*}{S_D^*} & \frac{\beta_T\phi_T S_{TL}^*}{S_D^*} & \frac{\beta_T\phi_T S_{TL}^*}{S_D^*} & 0 & 0 & 0 \\ \frac{\beta_T\phi_T S_{TN}^*}{S_D^*} & \frac{\beta_T\phi_T S_{TN}^*}{S_D^*} & \frac{\beta_T\phi_T S_{TN}^*}{S_D^*} & 0 & 0 & 0 \\ \frac{\beta_T\phi_T S_{TA}^*}{S_D^*} & \frac{\beta_T\phi_T S_{TA}^*}{S_D^*} & \frac{\beta_T\phi_T S_{TA}^*}{S_D^*} & 0 & 0 & 0 \end{pmatrix},$$

$$V = \begin{pmatrix} g_1 & 0 & 0 & 0 & 0 & 0 \\ -\sigma_D & g_2 & 0 & 0 & 0 & 0 \\ 0 & -\upsilon_D & g_3 & 0 & 0 & 0 \\ 0 & 0 & 0 & g_6 & 0 & 0 \\ 0 & 0 & 0 & -\alpha_L & g_8 & 0 \\ 0 & 0 & 0 & 0 & -\alpha_N & \mu_T \end{pmatrix}. \tag{24}$$

Therefore, using the definition of $\mathscr{R}_0 = \rho(FV^{-1})$, the $\mathscr{R}_0$ of the model is

$$\mathscr{R}_0 = \sqrt{\mathscr{R}_D \times \mathscr{R}_T}, \tag{25}$$

where ρ is the spectral radius and

$$\begin{aligned} \mathscr{R}_D &= \frac{\beta_D\phi_T\left(g_2g_3 + g_3\sigma_D + \sigma_D\upsilon_D\right)}{S_D^* g_1 g_2 g_3}, \\ \mathscr{R}_T &= \frac{\beta_T\phi_T\left[\left(g_8\mu_T + \alpha_L\alpha_N + \alpha_L\mu_T\right)S_{TL}^* + g_6\left(\alpha_N + \mu_T\right)S_{TN}^* + g_6g_8S_{TA}^*\right]}{g_6g_8\mu_T}. \end{aligned} \tag{26}$$

The expression $\mathscr{R}_D$ is the number of secondary infections in dogs. The expressions $\mathscr{R}_T$ is the number of secondary infections in ticks from a single infectious dog. Further, using Theorem 2 in [12], the following result is established.

Lemma 3. *The disease-free equilibrium (DFE) of the Ehrlichia chaffeensis model (14) is locally asymptotically stable (LAS) if* $\mathscr{R}_0 < 1$ *and unstable if* $\mathscr{R}_0 > 1$.

The basic reproduction number $\mathscr{R}_0$ is defined as the average number of new infections that result from one infectious individual (tick or dog) in a population that is fully susceptible [12–14]. The epidemiological significance of Lemma 3 is that *Ehrlichia chaffeensis* will be eliminated from within a herd if the reproduction number ($\mathscr{R}_0$) can be brought to (and maintained at) a value less than unity.

2.2. Sensitivity Analysis of Model (14). In order to determine the contribution of each of the model parameters to key model outputs (such as the number of infected), one can use a sensitivity analysis procedure [22–24]. Results of the sensitivity analysis help to identify the system parameters that are the best to target during an intervention, and also for future surveillance data gathering. We carried out a global sensitivity analysis using Latin Hypercube Sampling (LHS) and partial rank correlation coefficients (PRCC) to assess the impact of parameter uncertainty and the sensitivity of these key model outputs. The LHS method is a stratified sampling technique without replacement this allows for an efficient analysis of parameter variations across simultaneous uncertainty ranges in each parameter [25–28]. On the other hand, PRCC measures the strength of the relationship between the model outcome and the parameters, stating the degree of the effect that each parameter has on the model outcome [25–28].

We start by generating the LHS matrices and assuming all the model parameters are uniformly distributed. We then carry out a total of 1,000 simulations (runs) of the model for the LHS matrix, using the parameter values given in Table 2 (with ranges varying from ±20% of the stated baseline values) and as response functions, the sum of carries and infected. The parameter ranking using PRCC is then implemented following these simulation runs.

The outcome of the global sensitivity analysis is shown in Figure 2 and given in Table 3. The parameters with substantial effect on the sum of the acutely and chronically infected dogs are those parameters whose sensitivity index have significant p values less than or equal to 0.05. The parameters with the most impacts on $(A_D + C_D)$, are disease progression rate in dogs (σ_D), the rate (υ_D) dogs progress to chronic infection from acute infection, dog recovery rate (γ_D), the natural death rate of dogs (μ_D), death rate (δ_D) of acutely infected dogs, death rate of the chronically infected dogs (δ_C), birth rate of dogs (θ_D), the maturation rates eggs to larvae (α_E), the tick biting rate (ϕ_T), the dog transmission probability (β_D), the tick transmission probability (β_T) and death rate of ticks (μ_T), and the carrying capacity K. For the sum of infected larvae, nymphs, and adult ticks $(I_{TL} + I_{TN} + I_{TA})$, the significant parameters are υ_D, σ_D, μ_D, δ_D, δ_C, μ_E, α_E, ϕ_T, θ_D, β_T, and μ_T.

The PRCC index values of some of these parameters have positive signs while others have negative signs. The positive signs means that any increase in these parameters will lead to an increase in the response functions $(A_D + C_D$, and $I_{TL} + I_{TN} + I_{TA})$. While the negative signs implies increase in the parameters will lead to a decrease in the response functions. Hence, these parameters would be useful targets during mitigation efforts.

Therefore, control strategies which target those parameters with significant PRCC values will give the greatest impact on the model response functions. For instance, a control that aims for a 10% decrease in the transmission probability in dogs (β_D) will lead to 88% reduction in infected dogs $(A_D + C_D)$ and about 78% reduction in infected ticks $(I_{TL} + I_{TN} + I_{TA})$. Similarly a 10% decrease in the ticks transmission probability (β_T) will lead to 71.4% reduced infection in dogs and about 83% reduced infection in ticks. Also, a 10% deduction in tick biting rate (ϕ_T) will lead to about 95% reduction in infected dogs, and about 94% reduction in infected ticks. Furthermore, a 10% increase in ticks death rate (μ_T) will result in about 72.4% reduction in infected dogs and about 83.4% decrease in ticks.

3. Movement Model

Next, we extend the *Ehrlichia chaffeensis* model (6) by incorporating visitation and long distance migratory movements for dogs and ticks. Dogs are often taken to dog parks or on hiking by their owners, we capture these short dog movement through the visitation parameters p_{ij}, which is the proportion of time a dog in location i spends visiting location j [29, 30]. Ticks long distance migratory movement may be due to ticks dropping off after feeding on either migratory birds moving north or from white-tail deer or other larger mammals [31]. For the movement of dogs, we use the Lagrangian model, often use to model short term visitation between places [29, 32, 33]. For ticks movement on the other hand, we model their movement using Eulerian movement [34–36]. This kind of movement is used to model permanent migratory movement [37–39]. A number of mathematical models have used this approach to model tick movement [38, 39]. Thus, the movement model is given as

Table 2: Parameter values for each of the parameters for the *Ehrlichia chaffeensis* model (6).

Parameter	Description	Value (1/day)	Reference(s)
θ_D	Birth rate of dogs	70,000	[15]
γ_D	Rate of infected to recovered dogs	0.04761905	[2]
υ_D	Rate of acute to chronic infection in dogs	0.04761905	[2]
σ_D	Rate of exposed to infected dogs	0.07142857	[10]
ε	Rate of reinfection in dogs	0.00444444	[16]
α_E	Maturation rate from tick eggs to larvae	0.02439024	[17]
α_L	Maturation rate from tick larvae to nymphs	0.00273973	[17]
α_N	Maturation rate from nymphs to adult ticks	0.0037037	[17]
θ_A	Ticks egg laying rate	6000 eggs	[18]
μ_E	Death rate of tick eggs	0.008	[18]
μ_T	Death rate of ticks	0.003	[18]
μ_D	Natural death rate of dogs	0.00027397	[19]
δ_D	Acute infection death rate in dogs	0.1735	Assumed
δ_C	Chronic infection death rate in dogs	0.347	[20]
β_D	Dog transmission probability	0.152	[21]
ϕ_T	Tick biting rate	0.044	Assumed
β_T	Tick transmission probability	0.152	[21]

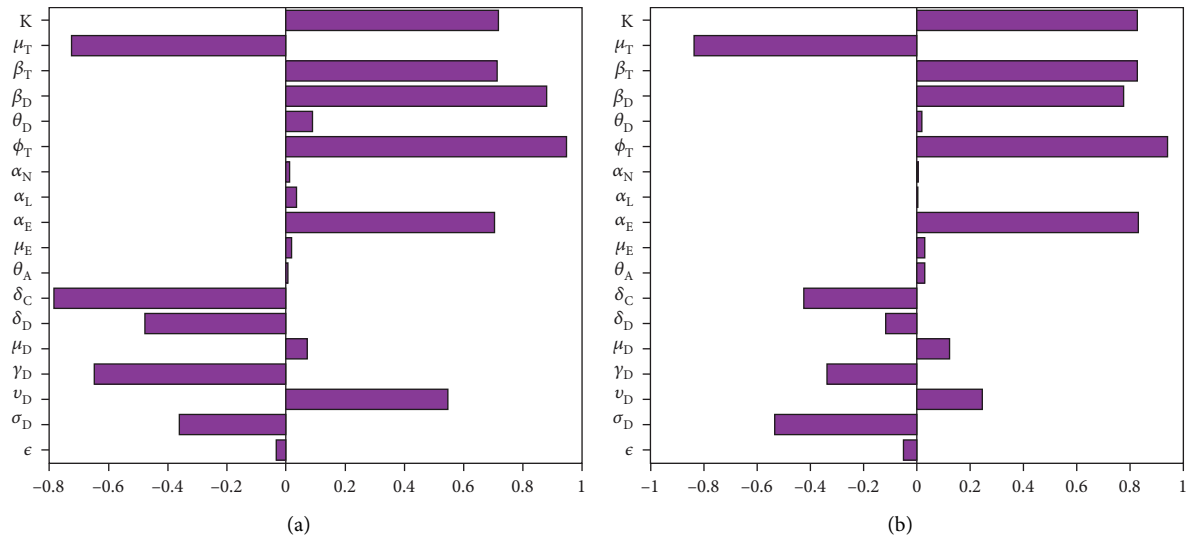

Figure 2: PRCC values for the *Ehrlichia chaffeensis* model (6), using as response functions: (a) the sum of infected dogs $(A_D + C_D)$; (b) the sum of infected ticks $(I_{TL} + I_{TN} + I_{TA})$. Using parameter values in Table 2 and ranges that ±20% from the baseline values.

Table 3: PRCC and p values of the *Ehrlichia chaffeensis* model (6) using as response functions the sum of infected dogs $(A_D + C_D)$ and the sum of infected tick $(I_{TL} + I_{TN} + I_{TA})$ with parameter values in Table 2 that are with ±20% ranges from the baseline values.

Parameters	$A_D + C_D$		$I_{TL} + I_{TN} + I_{TA}$	
	PRCC	p value	PRCC	p value
ε	−0.0335	0.2938	−0.0491	0.1242
σ_D	−0.3604	≤0.0001	−0.5323	≤0.0001
υ_D	0.5466	≤0.0001	0.2460	≤0.0001
γ_D	−0.6476	≤0.0001	−0.3367	≤0.0001
μ_D	0.0711	0.0258	0.1217	0.0001
δ_D	−0.4754	≤0.0001	−0.1163	0.0003
δ_C	−0.7851	≤0.0001	−0.4235	≤0.0001
θ_A	0.0051	0.8728	0.0300	0.3478
μ_E	0.0184	0.5642	0.0296	0.3544
α_E	0.7043	≤0.0001	0.8301	≤0.0001
α_L	0.0364	0.2548	0.0040	0.8991

Table 3: Continued.

Parameters	$A_D + C_D$		$I_{TL} + I_{TN} + I_{TA}$	
	PRCC	p value	PRCC	p value
α_N	0.0117	0.7142	0.0048	0.8815
ϕ_T	0.9484	0	0.9424	0
θ_D	0.0893	0.0051	0.0191	0.5488
β_D	0.8800	≤0.0001	0.7770	≤0.0001
β_T	0.7142	≤0.0001	0.8274	≤0.0001
μ_T	−0.7243	≤0.0001	−0.8346	≤0.0001
K	0.7164	≤0.0001	0.8271	≤0.0001

$$
\begin{aligned}
\frac{dS_D^i}{dt} &= \theta_D - \sum_{j=1}^{3} p_{ij}\frac{\beta_D\phi_T\left(I_{TL}^j + I_{TN}^j + I_{TA}^j\right)}{N_D^j}S_D^i - \mu_D S_D^i,\\
\frac{dE_D^i}{dt} &= \sum_{j=1}^{3} p_{ij}\frac{\beta_D\phi_T\left(I_{TL}^j + I_{TN}^j + I_{TA}^j\right)}{N_D^j}\left(S_D^i + \varepsilon R_D^i\right) - (\sigma_D + \mu_D)E_D^i,\\
\frac{dA_D^i}{dt} &= \sigma_D E_D^i - (\nu_D + \gamma_D + \mu_D + \delta_D)A_D^i,\\
\frac{dC_D^i}{dt} &= \nu_D A_D^i - (\mu_D + \delta_D)C_D^i,\\
\frac{dR_D^i}{dt} &= \gamma_D A_D^i - \sum_{j=1}^{3} p_{ij}\frac{\varepsilon\beta_D\phi_T\left(I_{TL}^j + I_{TN}^j + I_{TA}^j\right)}{N_D^j}R_D^i - \mu_D R_D^i,\\
\frac{dS_{TE}^i}{dt} &= \theta_A\left(1 - \frac{S_{TE}^i}{K^i}\right)\left(S_{TA}^i + I_{TA}^i\right) - (\sigma_E + \mu_E)S_{TE}^i,\\
\frac{dS_{TL}^i}{dt} &= \alpha_E S_{TE}^i - \frac{\beta_T^i\phi_T\left(E_D^i + A_D^i + C_D^i\right)}{N_D^i}S_{TL}^i - (\alpha_L + \mu_L)S_{TL}^i - \sum_{i\neq j}^{n} m_{ij}S_{TL}^i + \sum_{i\neq j}^{n} m_{ji}S_{TL}^j,\\
\frac{dI_{TL}^i}{dt} &= \frac{\beta_T^i\phi_T\left(E_D^i + A_D^i + C_D^i\right)}{N_D^i}S_{TL}^i - (\alpha_L + \mu_L)I_{TL}^i - \sum_{i\neq j}^{n} m_{ij}I_{TL}^i + \sum_{i\neq j}^{n} m_{ji}I_{TL}^j,\\
\frac{dS_{TN}^i}{dt} &= \alpha_L S_{TL}^i - \frac{\beta_T^i\phi_T\left(E_D^i + A_D^i + C_D^i\right)}{N_D^i}S_{TN}^i - (\alpha_N + \mu_N)S_{TN}^i - \sum_{i\neq j}^{n} m_{ij}S_{TN}^i + \sum_{i\neq j}^{n} m_{ji}S_{TN}^j,\\
\frac{dI_{TN}^i}{dt} &= \alpha_L I_{TL}^i + \frac{\beta_T^i\phi_T\left(E_D^i + A_D^i + C_D^i\right)}{N_D^i}S_{TN}^i - (\alpha_N + \mu_N)I_{TN}^i - \sum_{i\neq j}^{n} m_{ij}I_{TN}^i + \sum_{i\neq j}^{n} m_{ji}I_{TN}^j,\\
\frac{dS_{TA}^i}{dt} &= \alpha_N S_{TN}^i - \frac{\beta_T^i\phi_T\left(E_D^i + A_D^i + C_D^i\right)}{N_D^i}S_{TA}^i - \mu_A S_{TA}^i - \sum_{i\neq j}^{n} m_{ij}S_{TA}^i + \sum_{i\neq j}^{n} m_{ji}S_{TA}^j,\\
\frac{dI_{TA}^i}{dt} &= \alpha_N I_{TN}^i + \frac{\beta_T^i\phi_T\left(E_D^i + A_D^i + C_D^i\right)}{N_D^i}S_{TA}^i - \mu_A I_{TA}^i - \sum_{i\neq j}^{n} m_{ij}I_{TA}^i + \sum_{i\neq j}^{n} m_{ji}I_{TA}^j,
\end{aligned}
\tag{27}
$$

where $N_D^i = S_D^i + E_D^i + A_D^i + C_D^i + R_D^i$. We assumed all the model parameters values are the same in all the locations $i = 1, \ldots, n$, except for the carrying capacity (K^i), ticks death rate (μ_T^i), dog and tick transmission probabilities (β_D^i and β_T^i). The basic qualitative properties of the *Ehrlichia chaffeensis* model (7), the corresponding positivity analysis and

the boundedness of solutions are given in Appendix C. The stability analysis of the disease-free equilibrium (DFE) of model (7) leading to the associated reproduction number $\overline{\mathcal{R}}_0$ is given in Appendix D.

3.1. Sensitivity Analysis of Model (27) with Movement. To carry out global sensitivity analysis for the *Ehrlichia chaffeensis* model (27) with movement, we also use two response functions, the sum of infected dogs $(A_D^i + C_D^i)$ and the sum of infected ticks $(I_{TL}^i + I_{TN}^i + I_{TA}^i)$, $i = 1, 2, 3$. As with the case of model (14) above, we implemented the sensitivity analysis to determine the impact of the model parameters on these two response functions. We implemented the analysis using three different locations and considered two scenarios: (i) when the locations are isolated and (ii) when the locations are connected.

To carry out the sensitivity analysis, we fixed some parameters related to the natural history of the infection in dogs and ticks. We then assume the values of parameters like dog birth rate (θ_D^i), the carrying capacity (K^i), dogs and ticks transmission probabilities $(\beta_D^i$, and $\beta_T^i)$, and ticks death rate (μ_T^i) are location dependent since the different locations might have different climatic conditions or microclimates.

Figure 3 and Table 4 the results of the sensitivity analysis and the p values of the parameters for the case with no movement between the regions. The results show the parameters with the most impact on the sum of infected dogs $(A_D^i + C_D^i)$ and the sum of infected larvae, nymphs, and adult ticks $(I_{TL}^i + I_{TN}^i + I_{TA}^i)$. Observe that some parameters have positive PRCC values while others have negative values. Thus, the significant parameters are disease progression rate in dogs (σ_D), the rate (υ_D) dogs progress to chronic infection from acute infection, dog recovery rate (γ_D), the natural death rate of dogs (μ_D), death rate (δ_D) of acutely infected dogs, death rate of chronically infected dogs (δ_C), birth rate of dogs (θ_D^i), the maturation rates of eggs to larvae (α_E), the tick biting rate (ϕ_T), the dog transmission probability (β_D), the tick transmission probability (β_T^i) and death rate of ticks (μ_T^i), and the carrying capacity K^i. The PRCC values of parameters θ_D^i, K^i, β_D^i, β_T^i, and μ_T^i are relatively the same since there are no movement between the region.

Therefore, control strategies which target these parameters with significant PRCC values will give the greatest impact on the model response functions. For instance, a control that aims for a 10% decrease in the transmission probability in dogs (β_D^i) in the three locations will lead respectively to about 66.9%, 66.8%, and 67.0% reduction in infected dogs $(A_D^i + C_D^i)$ and to about 52.2%, 54.5%, and 56.9% reduction in infected ticks $(I_{TL}^i + I_{TN}^i + I_{TA}^i)$, respectively, in each of the locations. Similarly a 10% decrease in the ticks transmission probability (β_T) in each of the locations will lead to 43.7%, 42.6%, 43.5% reduced infection in dogs and about 60.2%, 59.5%, 59.3% reduced infection in ticks. Also, a 10% deduction in tick biting rate (ϕ_T) will lead to about 97.5% reduction in infected dogs, and 97.5% reduction in infected ticks. Note that an event that leads to 10% increase in these parameters would increase the number of infected dogs and ticks by these percentages in each of the locations.

However, a 10% increase in tick's death rate (μ_T) in each of the three locations would result in about 49.7%, 48.1%, 47.9% reduction in infected dogs and about 63.6%, 62.3%, 62.4% decrease in ticks. If on the other hand, tick's death rate decrease by 10% the infected dog and tick populations will increase by these percentages in each of the locations.

Figure 4 and Table 5 show the results of the sensitivity analysis and the p values of the parameters for the case with movement. Some of these parameters as with the isolated case have positive PRCC values while others have negative values. The significant parameters σ_D, υ_D, γ_D, μ_D, δ_D, δ_C, and α_E are relatively the same since we used the same parameters between the regions. On the other hand, the PRCC values of parameters θ_D^i, K^i, β_D^i, β_T^i, and μ_T^i are different, with those in location 1 having higher values than those in location 2 and 3 since there is more movement into location 1, than 2 and 3.

Therefore, control strategies which target those parameters with significant PRCC values will give the greatest impact on the model response functions. For instance, a control that aims for a 10% decrease in the transmission probability in dogs (β_D^i) in locations 1, 2, and 3 will lead to 49.8%, 49.5%, 31.1% reduction in infected dogs $(A_D^i + C_D^i)$ and about 65.8%, 37.9%, 17.3% reduction in infected ticks $(I_{TL}^i + I_{TN}^i + I_{TA}^i)$. Similarly a 10% decrease in the ticks transmission probability (β_T) in locations 1, 2, and 3 will lead to 67.9%, 26.8%, 12.5% reduced infection in dogs and about 86.2%, 47.2%, 17.7% reduced infection in ticks. Also, a 10% deduction in tick biting rate (ϕ_T) will lead to about 94.7% reduction in infected dogs, and about 97% reduction in infected ticks. Lastly, a 10% increase in ticks death rate (μ_T) in locations 1, 2, and 3 will result in about 50.7%, 27.5%, 8% reduction in infected dogs and about 77.1%, 50.6%, 18.1% decrease in ticks.

4. Simulating the *Ehrlichia chaffeensis* Model (27)

In this section, we would simulate the *Ehrlichia chaffeensis* model (27) when there are no movements between the three locations and when dogs and ticks move between the locations. Later on, we would use the results from the sensitivity analysis and simulate the *Ehrlichia chaffeensis* model (27) varying the transmission probabilities (β_D^i, β_T^i), and the ticks death rate (μ_T^i). Then, we would analyze the effect of these parameters on the spread of *Ehrlichia chaffeensis* separately and jointly.

We start by simulating model (27) with no movement using parameters given in Table 2. We assume that infection is higher in location 1, followed by location 2, and location 3 has the least infection. As expected Figures 5(a) and 5(b) show higher number of acutely and chronically infected dogs in location 1, followed by locations 2 and 3; higher infected larvae, nymphs, and adult ticks were also observed in Figures 5(c), 5(d), and 5(e) in location 1, followed by locations 2 and 3.

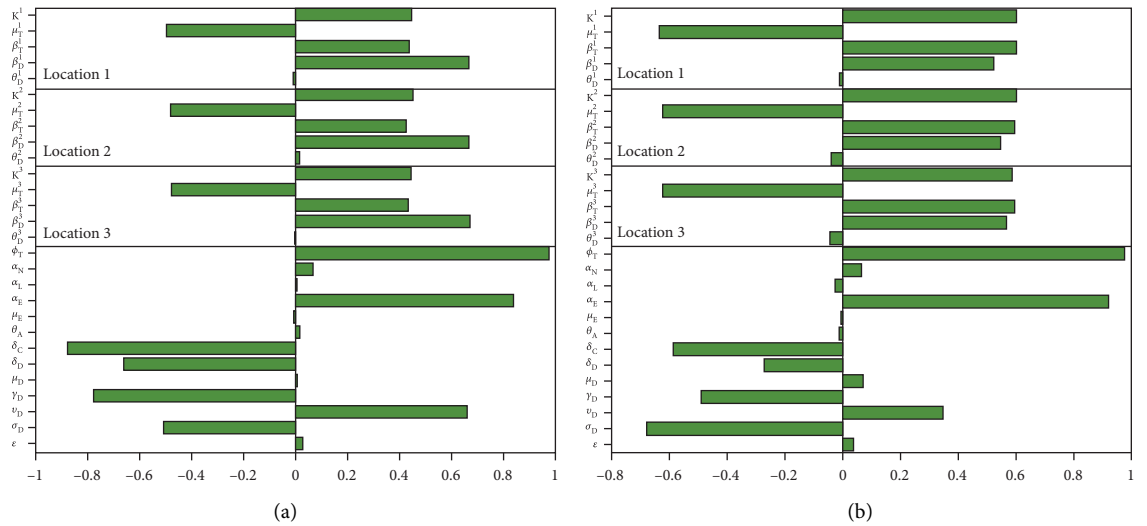

FIGURE 3: PRCC values for the *Ehrlichia chaffeensis* model (7) with no movement between the regions using as response functions: (a) the sum of infected dogs $(A_D^i + C_D^i)$; (b) the sum of infected ticks $(I_{TL}^i + I_{TN}^i + I_{TA}^i)$. Using parameter values in Table 2 and ranges that ±20% from the baseline values.

TABLE 4: PRCC and p values of the *Ehrlichia chaffeensis* model (7) with no movement between the regions using as response functions the sum of infected dogs $(A_D + C_D)$ and the sum of infected tick $(I_{TL} + I_{TN} + I_{TA})$ with parameter values in Table 2 that are with ±20% ranges from the baseline values.

Parameters	$A_D + C_D$		$I_{TL} + I_{TN} + I_{TA}$	
	PRCC	p value	PRCC	p value
ε	0.0279	0.3853	0.0378	0.2388
σ_D	−0.5088	≤0.0001	−0.6808	≤0.0001
υ_D	0.6599	≤0.0001	0.3462	≤0.0001
γ_D	−0.7750	≤0.0001	−0.4917	≤0.0001
μ_D	0.0037	0.9094	0.0704	0.0281
δ_D	−0.6603	≤0.0001	−0.2715	≤0.0001
δ_C	−0.8769	≤0.0001	−0.5871	≤0.0001
θ_A	0.0156	0.6265	−0.0128	0.6897
μ_E	−0.0048	0.8816	−0.0038	0.9058
α_E	0.8402	≤0.0001	0.9183	0
α_L	0.0032	0.9202	−0.0270	0.4003
α_N	0.0670	0.0365	0.0655	0.0410
ϕ_T	0.9747	0	0.9750	0
θ_D^3	−0.0008	0.9793	−0.0441	0.1698
β_D^3	0.6703	≤0.0001	0.5685	≤0.0001
β_T^3	0.4351	≤0.0001	0.5932	≤0.0001
μ_T^3	−0.4789	≤0.0001	−0.6239	≤0.0001
K^3	0.4471	≤0.0001	0.5875	≤0.0001
θ_D^2	0.0169	0.5978	−0.0382	0.2340
β_D^2	0.6680	≤0.0001	0.5452	≤0.0001
β_T^2	0.4263	≤0.0001	0.5951	≤0.0001
μ_T^2	−0.4809	≤0.0001	−0.6248	≤0.0001
K^2	0.4538	≤0.0001	0.6034	≤0.0001
θ_D^1	−0.0074	0.8167	−0.0102	0.7496
β_D^1	0.6688	≤0.0001	0.5217	≤0.0001
β_T^1	0.4372	≤0.0001	0.6020	≤0.0001
μ_T^1	−0.4968	≤0.0001	−0.6358	≤0.0001
K^1	0.4457	≤0.0001	0.6019	≤0.0001

With this movement scenario, the locations are isolated with no movement between them.

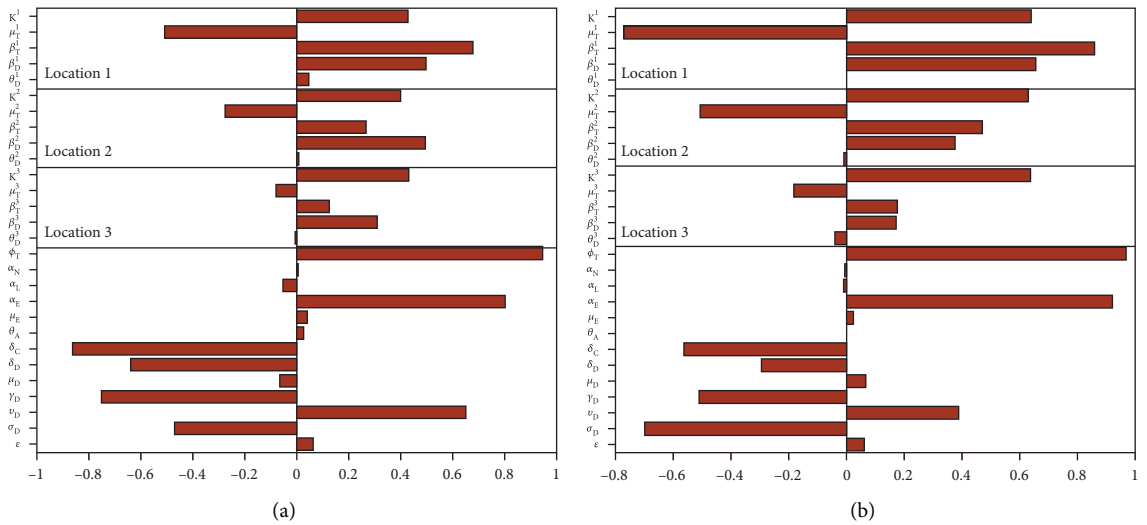

FIGURE 4: PRCC values for the *Ehrlichia chaffeensis* model (7) with movement between the regions using as response functions: (a) the sum of infected dogs $(A_D^i + C_D^i)$; (b) the sum of infected ticks $(I_{TL}^i + I_{TN}^i + I_{TA}^i)$. Using parameter values in Table 2 and ranges that ±20% from the baseline values. Under this scenario, there is increased movement to location 1, than 2 and 3. Location 3 has the least movement into it.

TABLE 5: PRCC and p values of the *Ehrlichia chaffeensis* model (27) with movement between the regions using as response functions the sum of infected dogs $(A_D + C_D)$ and the sum of infected tick $(I_{TL} + I_{TN} + I_{TA})$ with parameter values in Table 2 that are with ±20% ranges from the baseline values.

Parameters	$A_D + C_D$		$I_{TL} + I_{TN} + I_{TA}$	
	PRCC	p value	PRCC	p value
ϵ	0.0638	0.0468	0.0618	0.0539
σ_D	−0.4702	≤0.0001	−0.7006	≤0.0001
υ_D	0.6496	≤0.0001	0.3912	≤0.0001
γ_D	−0.7530	≤0.0001	−0.5108	≤0.0001
μ_D	−0.0645	0.0444	0.0683	0.0331
δ_D	−0.6403	≤0.0001	−0.2912	≤0.0001
δ_C	−0.8629	≤0.0001	−0.5626	≤0.0001
θ_A	0.0283	0.3772	0.0023	0.9437
μ_E	0.0416	0.1947	0.0250	0.4360
α_E	0.8030	≤0.0001	0.9235	0
α_L	−0.0527	0.1001	−0.0071	0.8241
α_N	0.0036	0.9112	−0.0035	0.9125
ϕ_T	0.9466	0	0.9695	0
θ_D^3	−0.0070	0.8269	−0.0396	0.2172
β_D^3	0.3107	≤0.0001	0.1731	≤0.0001
β_T^3	0.1252	0.0001	0.1774	≤0.0001
μ_T^3	−0.0801	0.0125	−0.1810	≤0.0001
K^3	0.4308	≤0.0001	0.6394	≤0.0001
θ_D^2	0.0066	0.8367	−0.0083	0.7971
β_D^2	0.4950	≤0.0001	0.3786	≤0.0001
β_T^2	0.2678	≤0.0001	0.4716	≤0.0001
μ_T^2	−0.2749	≤0.0001	−0.5064	≤0.0001
K^2	0.4011	≤0.0001	0.6311	≤0.0001
θ_D^1	0.0476	0.1378	0.0014	0.9646
β_D^1	0.4981	≤0.0001	0.6585	≤0.0001
β_T^1	0.6794	≤0.0001	0.8616	≤0.0001
μ_T^1	−0.5074	≤0.0001	−0.7708	≤0.0001
K^1	0.4292	≤0.0001	0.6408	≤0.0001

With the movement scenario, the locations are connected.

Next, we simulate model (27) with more movement into location 3 and least movement into locations 1 while infection remain higher in location 1 and smallest in location 3. With this scenario, Figures 6(a) and 6(b) show higher number of acutely and chronically infected dogs in location 3, followed by locations 2 then 1 even though infection is

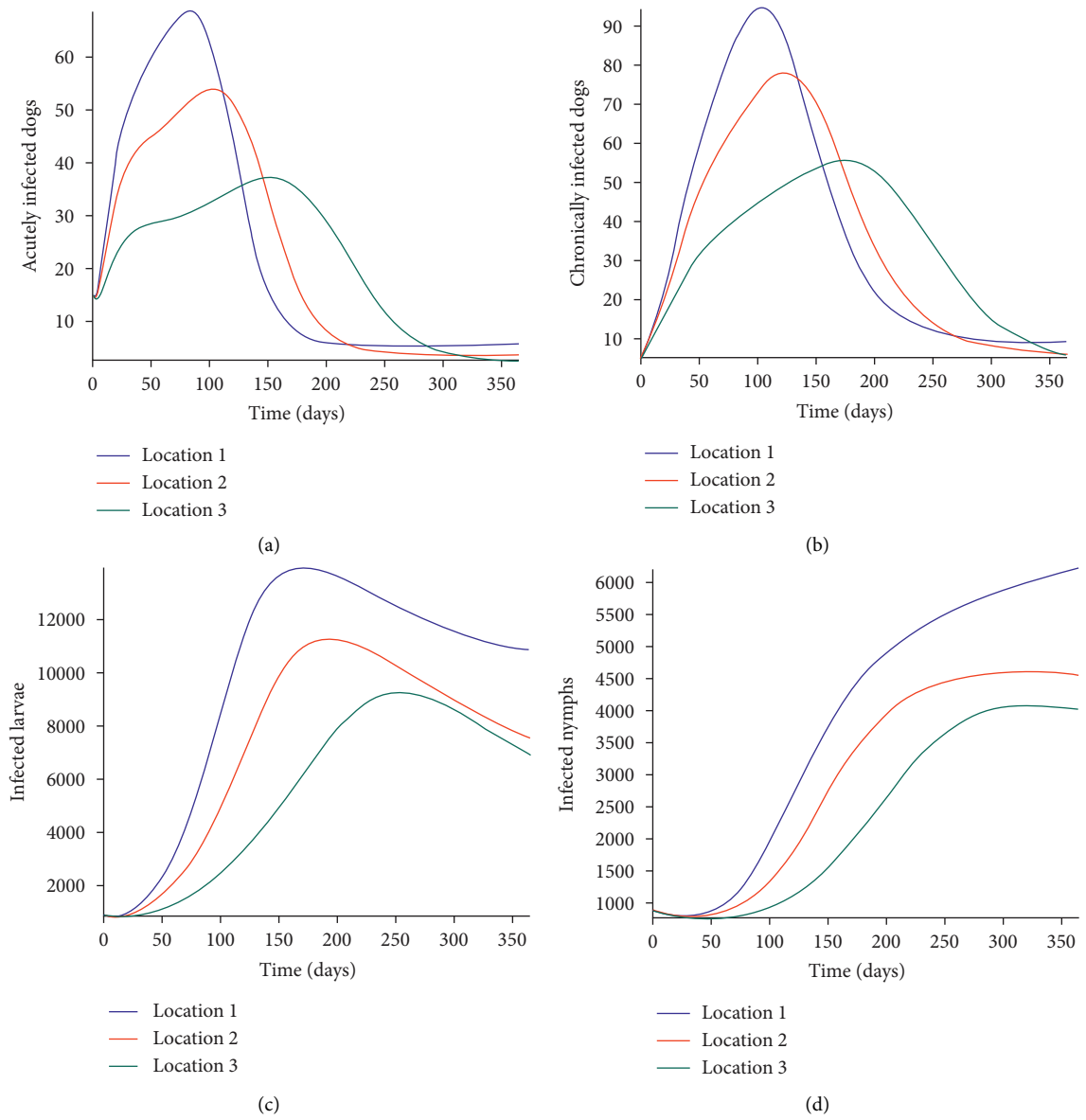

Figure 5: Continued.

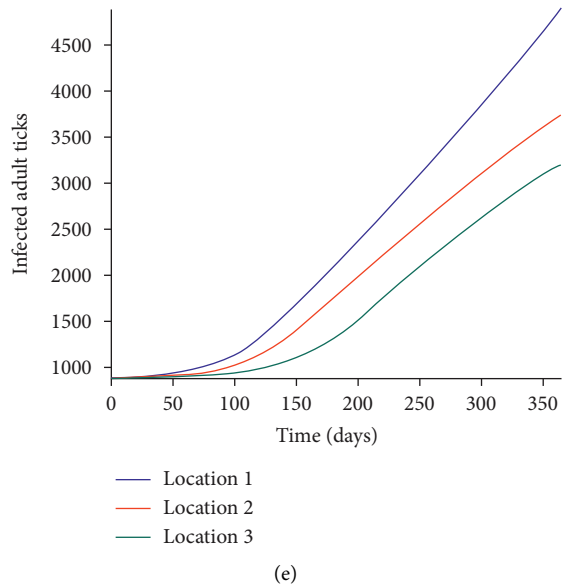

(e)

FIGURE 5: Simulation results of model (7) with no movement using parameters given in Table 2. Infection is higher in location 1, followed by location 2, location 3 has the least infection. (a) Acutely infected dogs; (b) chronically infected dogs; (c) infected larvae; (d) Infected nymphs; (e) infected adult ticks.

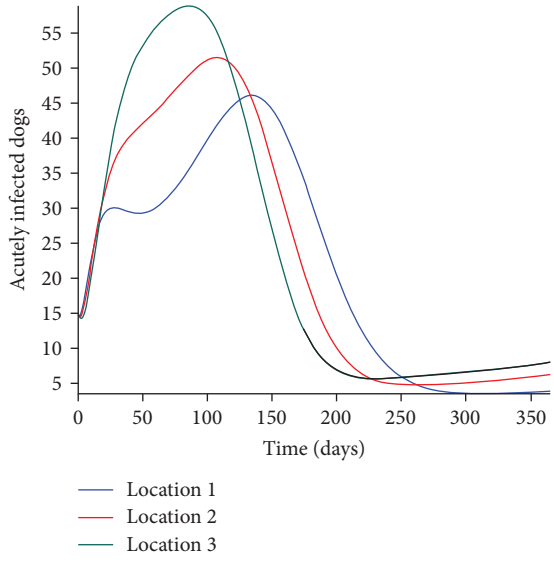

(a)

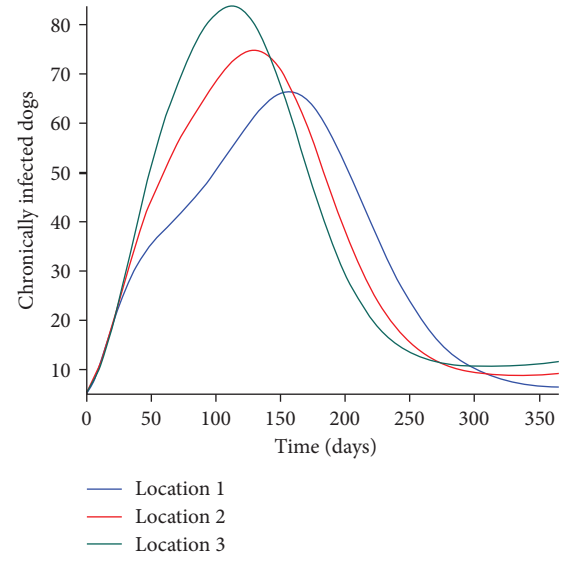

(b)

FIGURE 6: Continued.

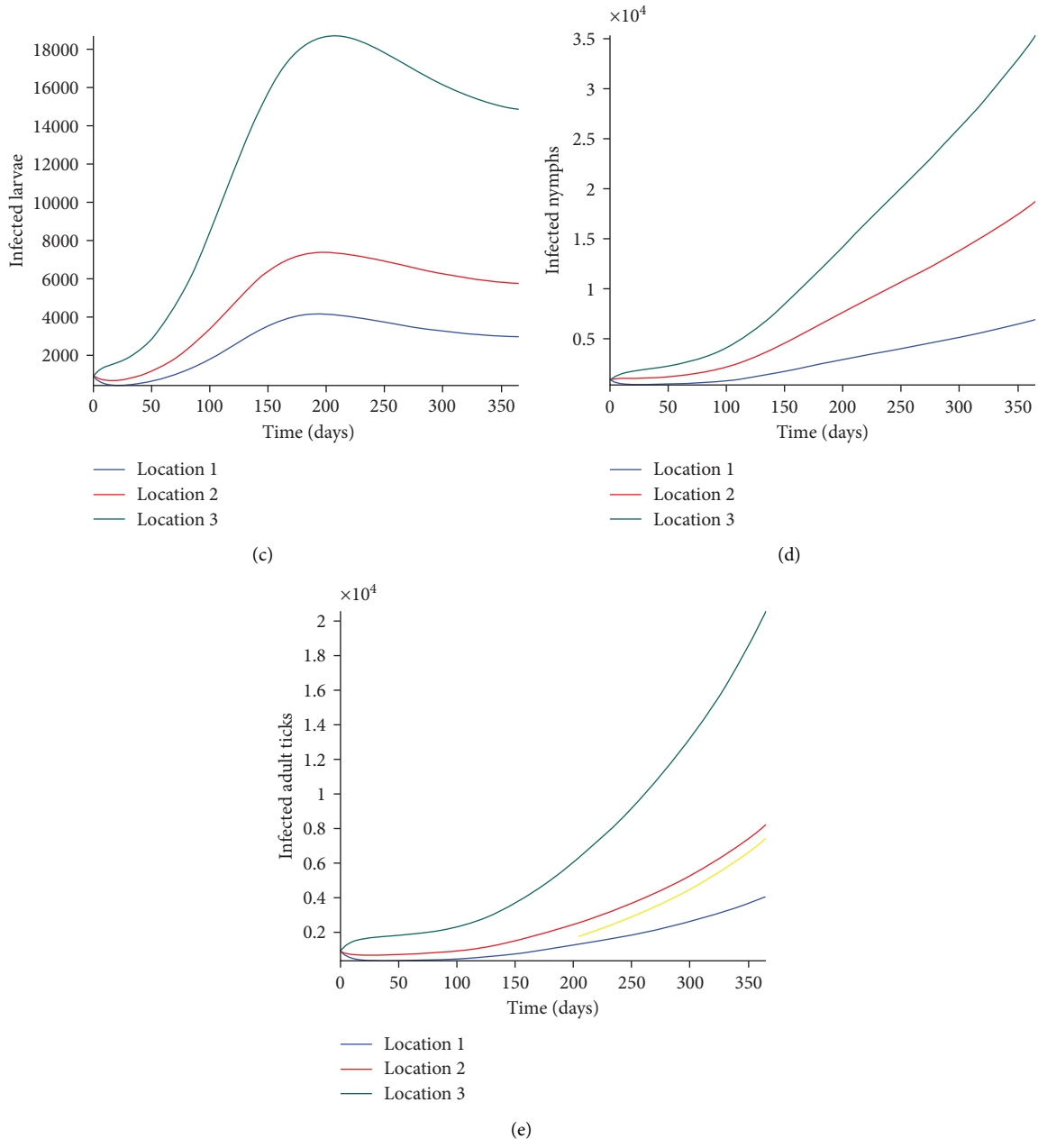

Figure 6: Simulation results of model (7) with movement using parameters given in Table 2. Infection is higher in location 1, followed by location 2, location 3 has the least infection. More movement to location 3 from locations 1, and 3. (a) Acutely infected dogs; (b) chronically infected dogs; (c) infected larvae; (d) infected nymphs; (e) infected adult ticks.

higher in location 1. Also, higher infected larvae, nymphs, and adult ticks were observed in location 3, followed by locations 2 and 1, see Figures 6(c), 6(d), and 6(e).

These results show the impact of movement on the transmission of the disease as dogs and ticks move across regions.

In the next section, we would use the results from the sensitivity analysis and simulate the *Ehrlichia chaffeensis* model (27) varying the transmission probabilities (β_D^i, β_T^i) and the ticks' death rate (μ_T^i). We analyze jointly the effect of these parameters on the spread of *Ehrlichia chaffeensis* within the dogs and ticks populations. Note that it makes sense to explore the joint effect of these parameters since the outcome of the sensitivity analysis is only on the effect of one parameter at a time.

4.1. Effect of Disease Transmission and Ticks Natural Death. Here, we investigate the impact of disease transmission probabilities and the ticks death rate as control measures on infected dogs and ticks. We vary the values of the transmission probabilities (β_D^i, β_T^i) and the number of ticks death rate (μ_T^i) and then examine the effect of these measures separately and jointly on the trajectories of

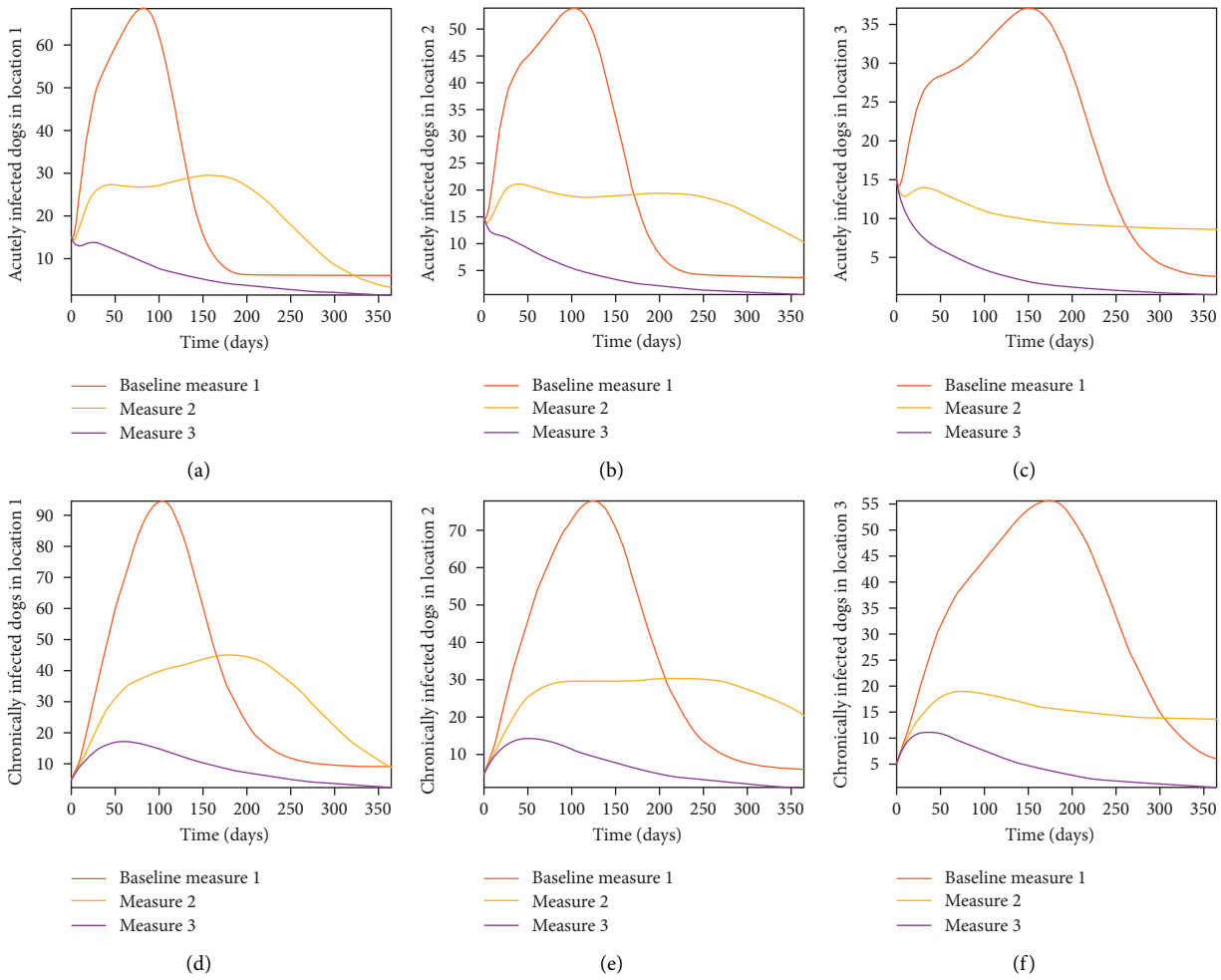

Figure 7: Simulation results of model (7) with no movement using parameters given in Table 2. Infection is higher in location 1, followed by location 2, location 3 has the least infection. More movement to location 3 from locations 1 and 3. (a–c) acutely infected dogs; (d–f) chronically infected dogs.

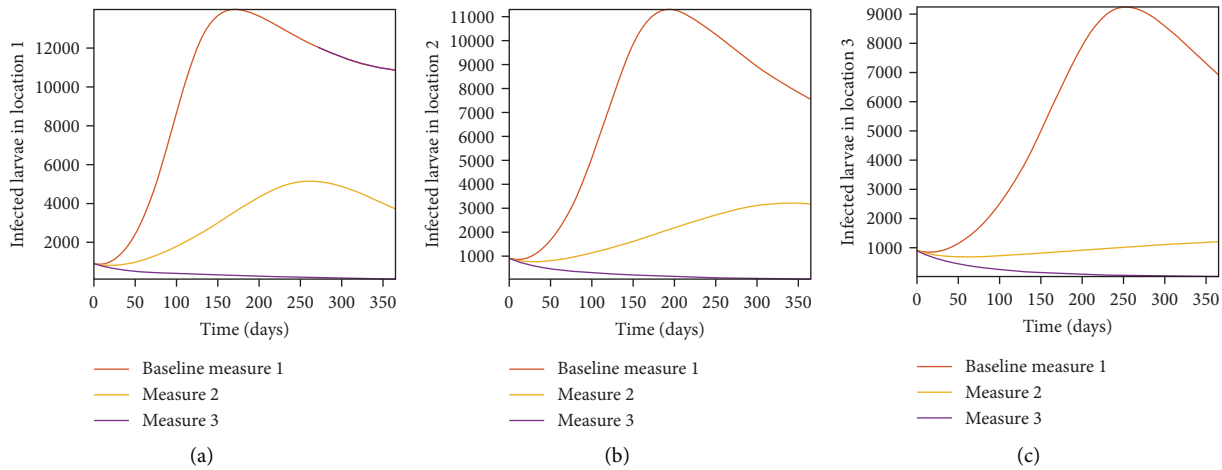

Figure 8: Continued.

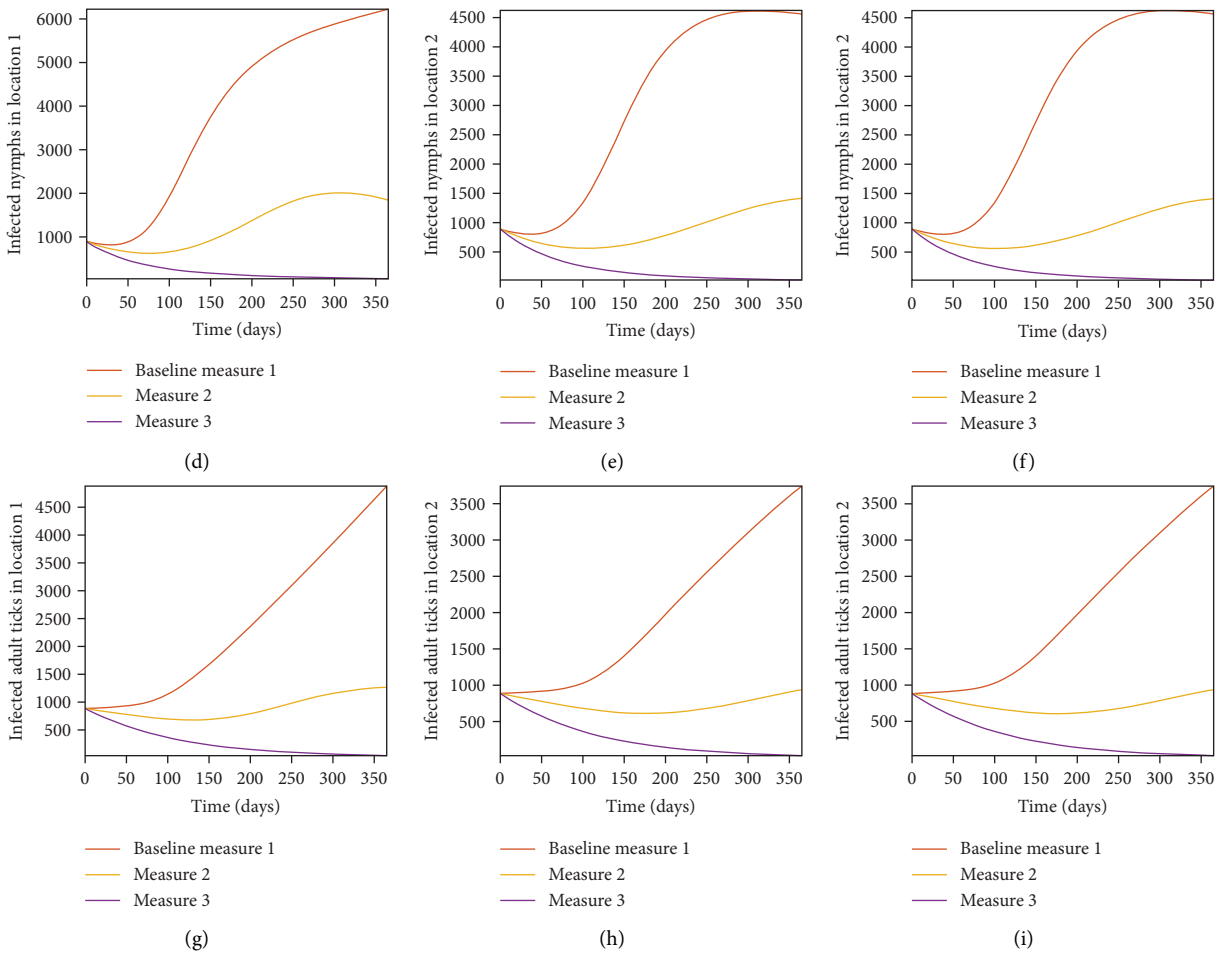

Figure 8: Simulation results of model (27) with no movement using parameters given in Table 2. Infection is higher in location 1, followed by location 2, location 3 has the least infection. More movement to location 3 from locations 1 and 3. (a–c) infected larvae; (d–f) infected nymphs; (g–i) infected adult ticks.

Table 6: Sum of the simulation of model (27) with no movement into the different locations using three different control measures.

Measures	Location 1		Location 2		Location 3	
1	A_D^1	8.6860×10^5	A_D^2	8.1537×10^5	A_D^3	7.6898×10^5
2	A_D^1	7.4407×10^5	A_D^2	6.5097×10^5	A_D^3	3.7349×10^5
3	A_D^1	1.9840×10^5	A_D^2	1.4660×10^5	A_D^3	9.6643×10^4
1	C_D^1	1.3523×10^6	C_D^2	1.2787×10^6	C_D^3	1.2063×10^6
2	C_D^1	1.1570×10^6	C_D^2	9.7318×10^5	C_D^3	5.5894×10^5
3	C_D^1	3.2066×10^5	C_D^2	2.4321×10^5	C_D^3	1.6682×10^5
1	I_{TL}^1	3.5822×10^8	I_{TL}^2	2.6880×10^8	I_{TL}^3	2.0342×10^8
2	I_{TL}^1	1.1852×10^8	I_{TL}^2	7.2714×10^7	I_{TL}^3	3.3064×10^7
3	I_{TL}^1	1.1374×10^7	I_{TL}^2	8.7850×10^6	I_{TL}^3	7.2365×10^6
1	I_{TN}^1	1.4126×10^8	I_{TN}^2	1.0978×10^8	I_{TN}^3	8.6427×10^7
2	I_{TN}^1	4.7045×10^7	I_{TN}^2	3.1790×10^7	I_{TN}^3	1.8848×10^7
3	I_{TN}^1	8.0034×10^6	I_{TN}^2	7.3395×10^6	I_{TN}^3	6.9439×10^6
1	I_{TA}^1	8.5854×10^7	I_{TA}^2	7.1381×10^7	I_{TA}^3	6.0548×10^7
2	I_{TA}^1	3.2641×10^7	I_{TA}^2	2.6498×10^7	I_{TA}^3	2.1308×10^7
3	I_{TA}^1	9.6459×10^6	I_{TA}^2	9.4308×10^6	I_{TA}^3	9.3019×10^6

Measure 1: used the baseline parameters for β_D^i, β_T^i and μ_T^i, $i = 1, 2, 3$, as given in Table 2. Measure 2: the parameters for β_D^i, β_T^i, are divided by two and μ_T^i are doubled. Measure 3: β_D^i, β_T^i, values are divided by four and μ_T^i are multiplied by four.

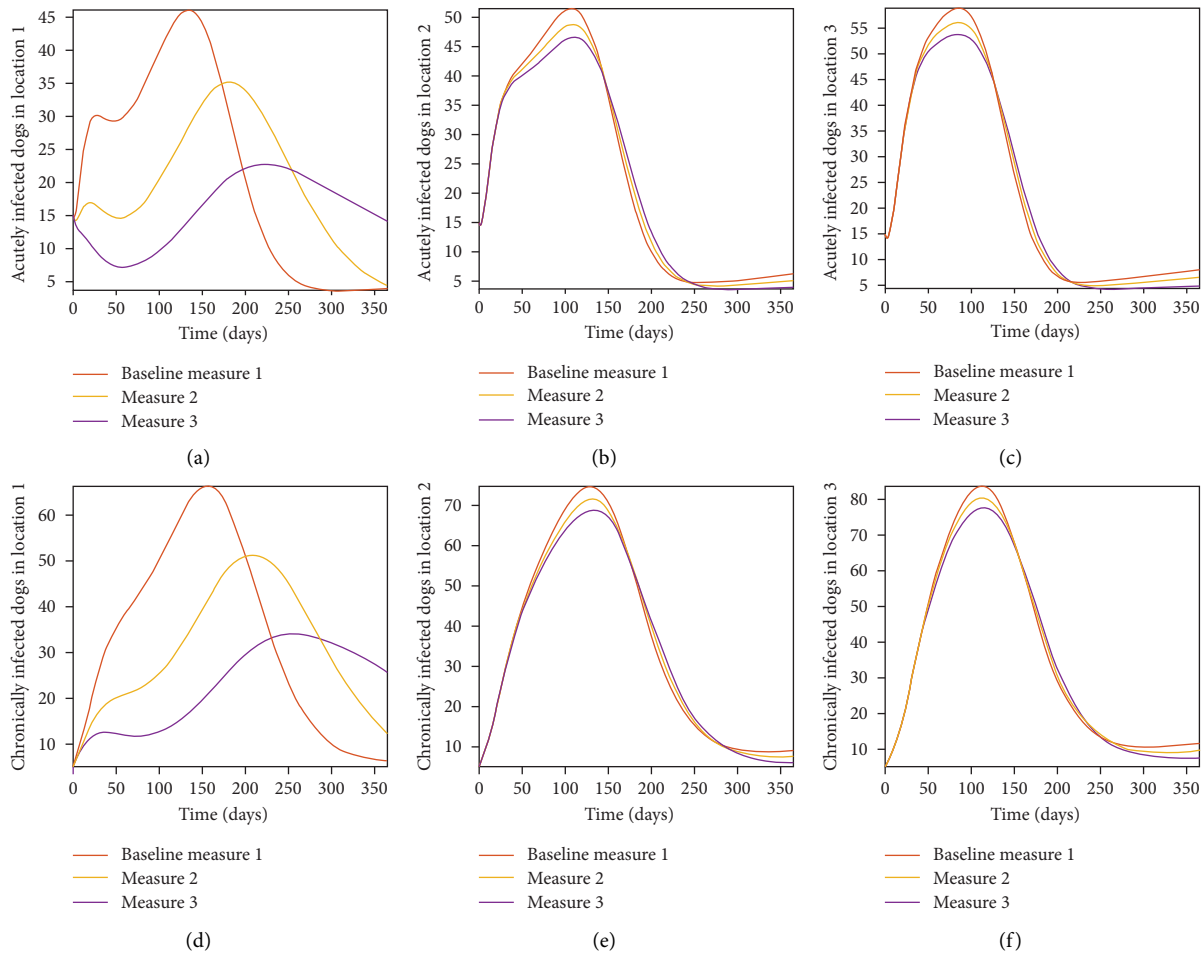

Figure 9: Simulation results of model (7) with movement. Control measures are only implemented in location 1. (a)–(c) acutely infected dogs; (d)–(f) chronically infected dogs.

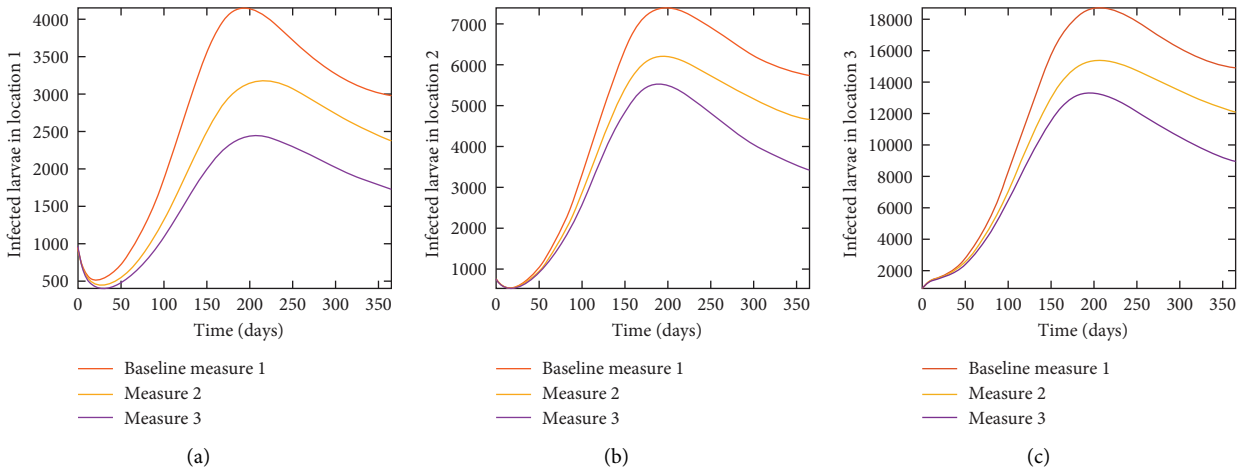

Figure 10: Continued.

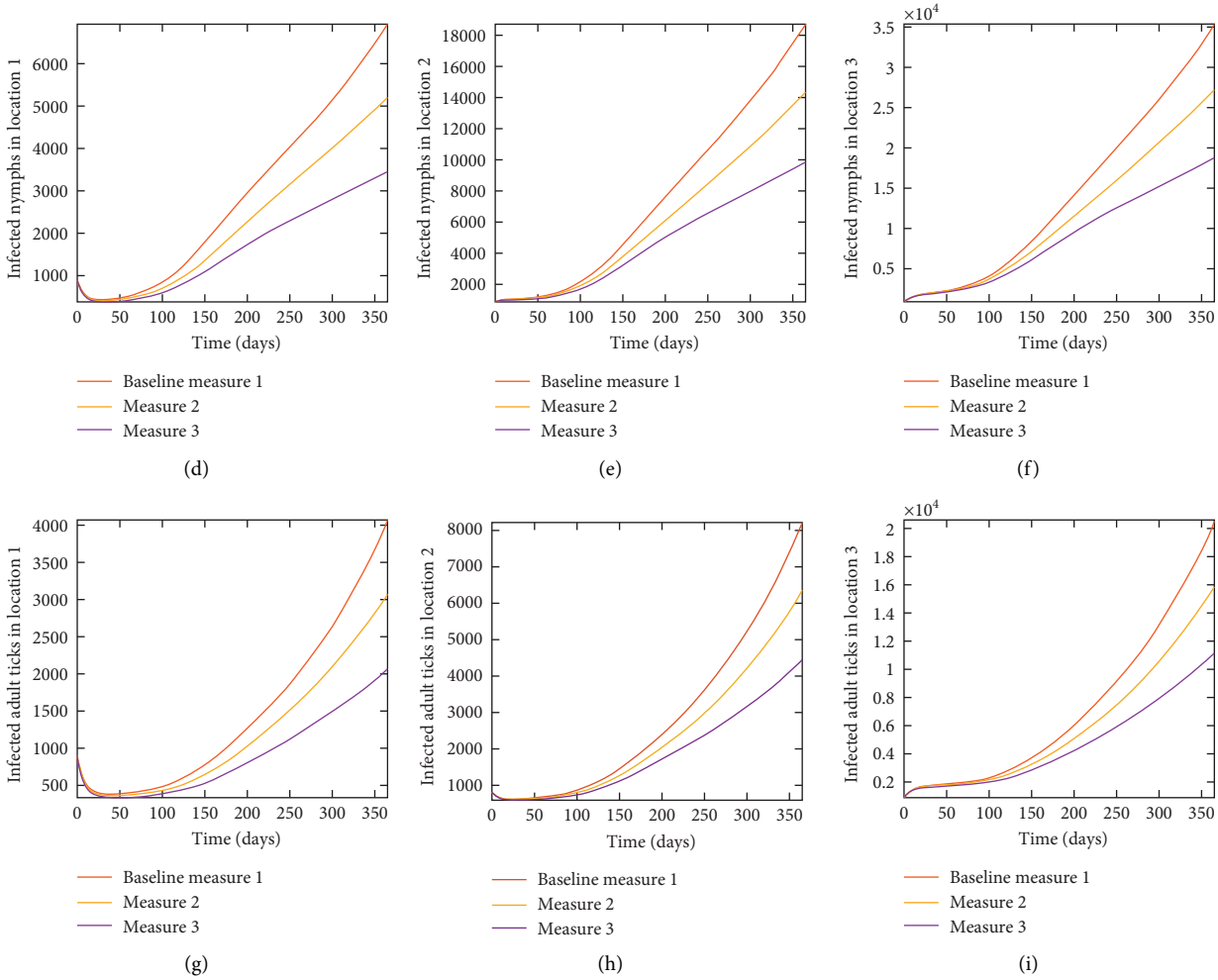

FIGURE 10: Simulation results of model (27) with movement. Control measures are implemented in location 1 only. (a–c) infected larvae; (d–f) infected nymphs; (g–i) infected adult ticks.

TABLE 7: Sum of the simulation results of model (7) with movement.

Measures	Location 1		Location 2		Location 3	
1	A_D^1	7.8998×10^5	A_D^2	8.2910×10^5	A_D^3	8.6320×10^5
2	A_D^1	7.3806×10^5	A_D^2	8.1344×10^5	A_D^3	8.4190×10^5
3	A_D^1	5.7417×10^5	A_D^2	7.9930×10^5	A_D^3	8.2301×10^5
1	C_D^1	1.2379×10^6	C_D^2	1.2905×10^6	C_D^3	1.3359×10^6
2	C_D^1	1.1365×10^6	C_D^2	1.2705×10^6	C_D^3	1.3089×10^6
3	C_D^1	8.3462×10^5	C_D^2	1.2531×10^6	C_D^3	1.2859×10^6
1	I_{TL}^1	9.8522×10^7	I_{TL}^2	1.8229×10^8	I_{TL}^3	4.6149×10^8
2	I_{TL}^1	7.5886×10^7	I_{TL}^2	1.5423×10^7	I_{TL}^3	3.8438×10^8
3	I_{TL}^1	5.7685×10^7	I_{TL}^2	1.3168×10^6	I_{TL}^3	3.2258×10^8
1	I_{TN}^1	1.0240×10^8	I_{TN}^2	2.7218×10^8	I_{TN}^3	5.1081×10^8
2	I_{TN}^1	7.9835×10^7	I_{TN}^2	2.1841×10^8	I_{TN}^3	4.1087×10^8
3	I_{TN}^1	5.8344×10^7	I_{TN}^2	1.6843×10^8	I_{TN}^3	3.1871×10^8
1	I_{TA}^1	5.2300×10^7	I_{TA}^2	1.0372×10^8	I_{TA}^3	2.5791×10^8
2	I_{TA}^1	4.2156×10^7	I_{TA}^2	8.6180×10^7	I_{TA}^3	2.1335×10^8
3	I_{TA}^1	3.1419×10^7	I_{TA}^2	6.8570×10^7	I_{TA}^3	1.6840×10^8

Control measures are only implemented in location 1.

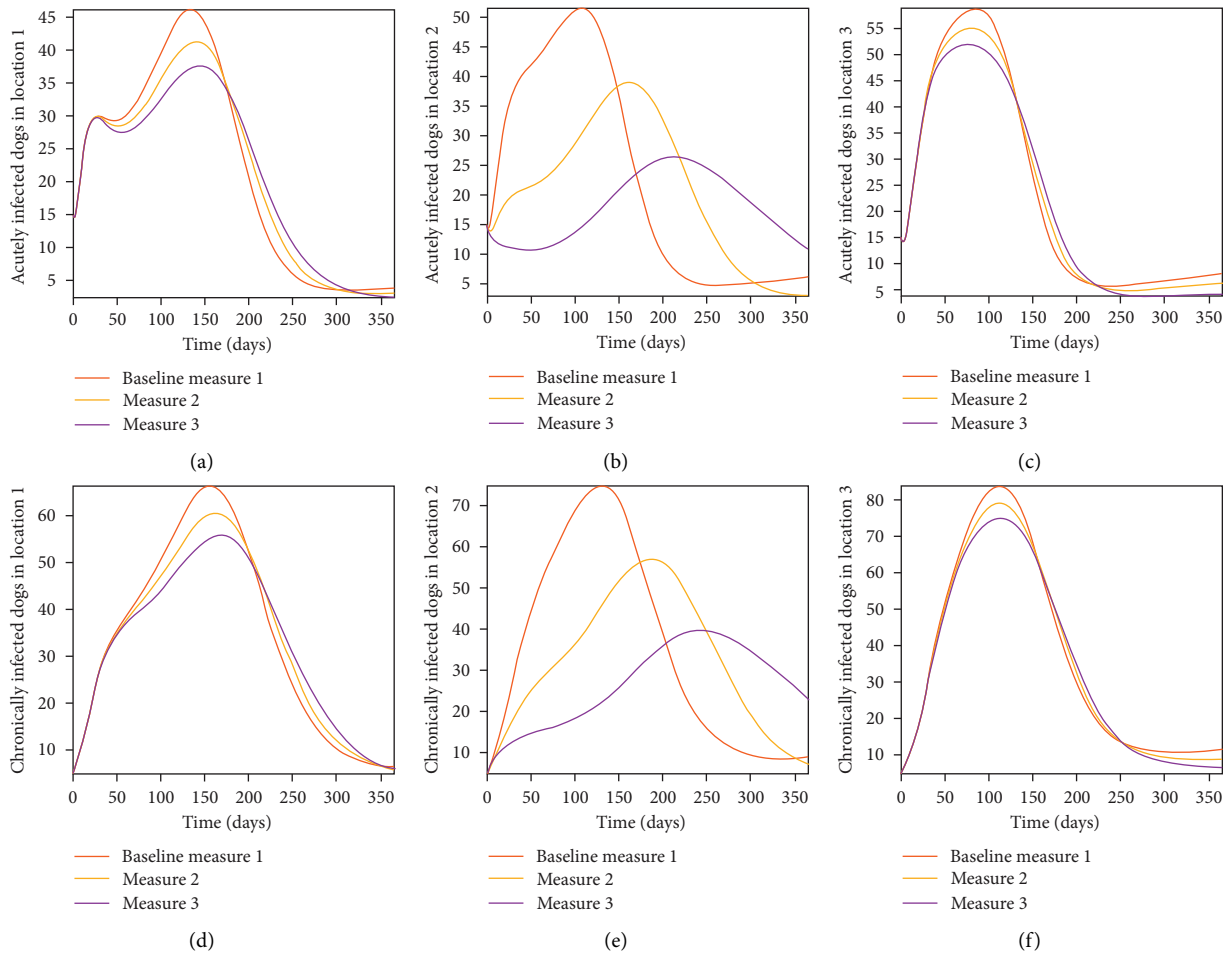

Figure 11: Simulation results of model (7) with movement. Control measures are only implemented in location 2. (a)–(c) acutely infected dogs; (d)–(f) chronically infected dogs.

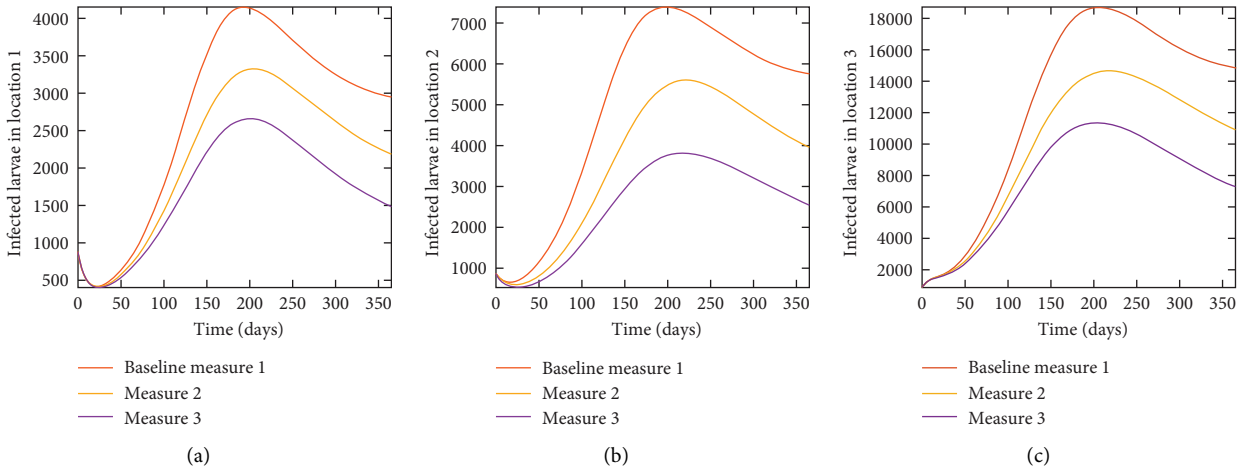

Figure 12: Continued.

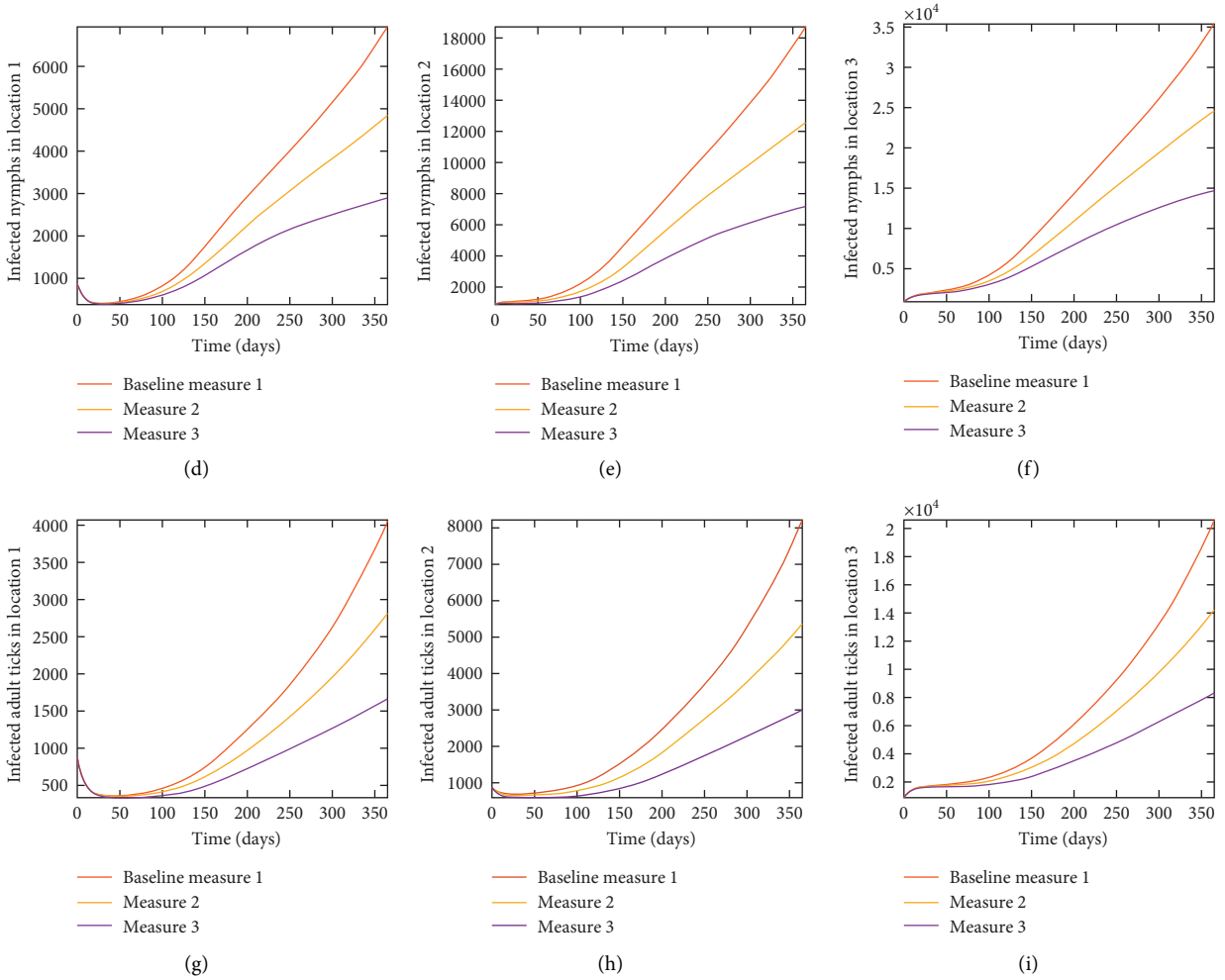

FIGURE 12: Simulation results of model (27) with movement. Control measures are implemented in location 2 only. (a–c) infected larvae; (d–f) infected nymphs; (g–i) infected adult ticks.

TABLE 8: Sum of the simulation results of model (7) with movement.

Measures	Location 1		Location 2		Location 3	
1	A_D^1	7.8998×10^5	A_D^2	8.2910×10^5	A_D^3	8.6320×10^5
2	A_D^1	7.7723×10^5	A_D^2	7.6326×10^5	A_D^3	8.3576×10^5
3	A_D^1	7.6435×10^5	A_D^2	6.5388×10^5	A_D^3	8.1033×10^5
1	C_D^1	1.2379×10^6	C_D^2	1.2905×10^6	C_D^3	1.3359×10^6
2	C_D^1	1.2197×10^6	C_D^2	1.1930×10^6	C_D^3	1.3011×10^6
3	C_D^1	1.1996×10^6	C_D^2	9.6952×10^5	C_D^3	1.2695×10^6
1	I_{TL}^1	9.8522×10^7	I_{TL}^2	1.8229×10^8	I_{TL}^3	4.6149×10^8
2	I_{TL}^1	7.9056×10^7	I_{TL}^2	1.3233×10^8	I_{TL}^3	3.6249×10^8
3	I_{TL}^1	6.2368×10^7	I_{TL}^2	9.1858×10^7	I_{TL}^3	2.7911×10^8
1	I_{TN}^1	1.0240×10^8	I_{TN}^2	2.7218×10^8	I_{TN}^3	5.1081×10^8
2	I_{TN}^1	7.7780×10^7	I_{TN}^2	1.9816×10^8	I_{TN}^3	3.8444×10^8
3	I_{TN}^1	5.4568×10^7	I_{TN}^2	1.2939×10^8	I_{TN}^3	2.6622×10^8
1	I_{TA}^1	5.2300×10^7	I_{TA}^2	1.0372×10^8	I_{TA}^3	2.5791×10^8
2	I_{TA}^1	4.0332×10^7	I_{TA}^2	7.6112×10^7	I_{TA}^3	1.9685×10^8
3	I_{TA}^1	2.8382×10^7	I_{TA}^2	4.9422×10^7	I_{TA}^3	1.3647×10^8

Control measures are only implemented in location 2.

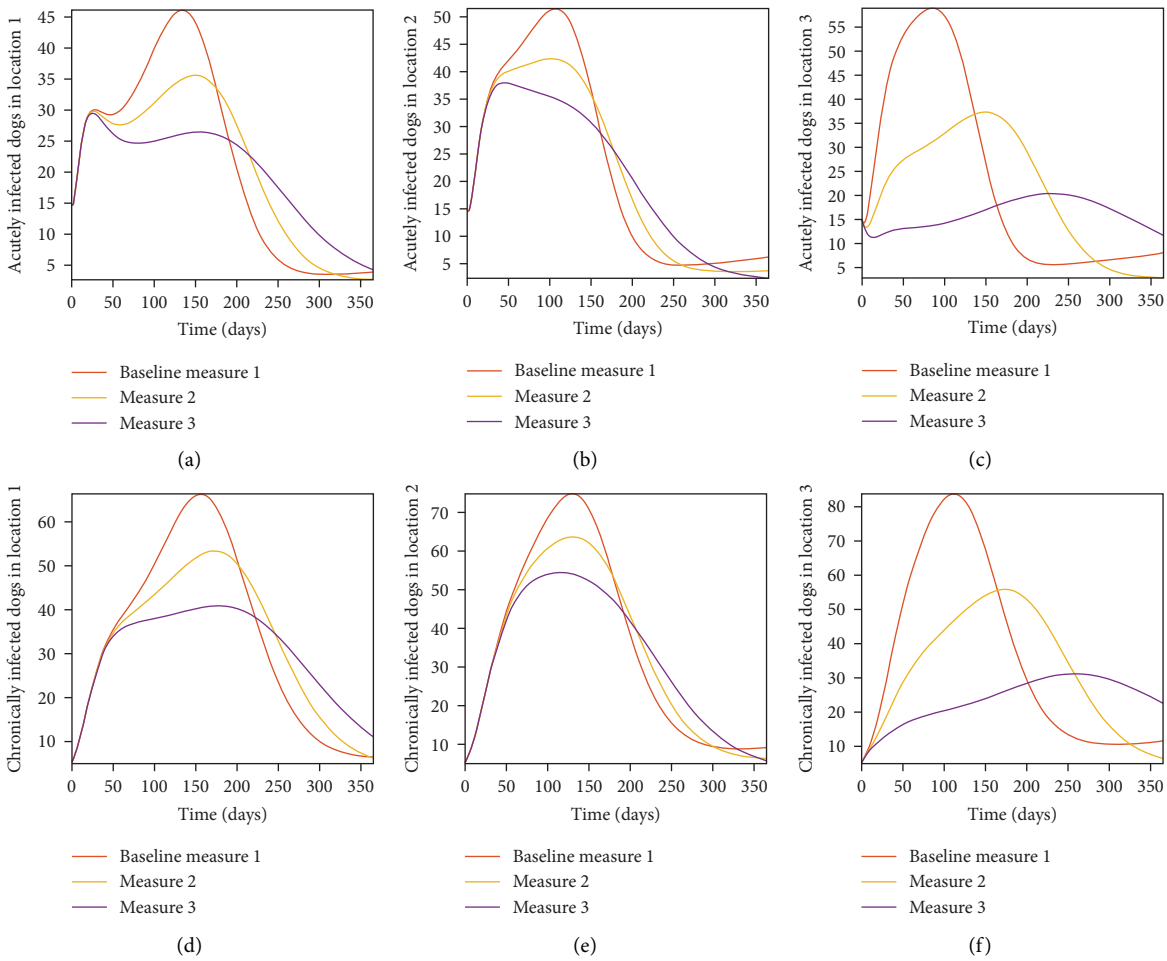

FIGURE 13: Simulation results of model (7) with movement. Control measures are only implemented in location 3. (a)–(c) acutely infected dogs; (d)–(f) chronically infected dogs.

infected dogs and ticks under several scenarios (i) when the three locations are isolated with no movement between them and control measures are implemented in each location and (ii) when the locations are connected with movement between and control measures are first implemented a location at a time and then implemented at once in all the locations.

4.2. Isolated Locations: Disease Transmission and Ticks Control. Here, we explore the combined effect of varying the transmission probabilities (β_D^i, and β_T^i) and ticks natural death rate (μ_T^i) when there are no movements between the locations. However, infection is higher in location 1, followed by location 2, location 3 has the least infection. We considered three measures: (i) Measure 1 where the baseline parameters are used for β_D^i, β_T^i, and $\mu_T^i, i = 1, 2, 3$, as given in Table 2; (ii) Measure 2, the baseline parameter values for β_D^i, β_T^i, are halved while the value for μ_T^i is doubled; and (iii) Measure 3, the baseline parameter values for β_D^i, β_T^i are divided by four while the values for μ_T^i are multiplied by four.

In Figure 7, we observed reduction in acutely and chronically infected dogs in each location as the control measures varies as described above; Figure 8 show the infected larvae, nymphs, and adult ticks in each locations. Table 6 show similar trends with the sum of the acutely and chronically infected dogs and ticks over the simulation period of 52 weeks representing a year.

This results show the importance of ensuring the infection rates are low in order to reduce the overall burden of the disease in each location.

4.3. Connected Locations: Control in One Location at a Time. In this section, we explore the effect of varying the transmission probabilities (β_D^i, and β_T^i) and ticks natural death rate (μ_T^i) when dogs and ticks can move freely between the locations. We assume the infection is higher in location 1, followed by locations 2, and 3; location 3 has the least infection. Here, we consider the scenario where the control measures are implemented a location at a time. We also considered three control measures 1,2, 3: with Measure 1, the baseline parameter values are used for β_D^i, β_T^i, and $\mu_T^i, i = 1, 2, 3$, as given in Table 2; with Measure 2, the baseline parameter values for β_D^i, β_T^i, are halved while and μ_T^i is doubled; with Measure 3, the baseline parameter values for β_D^i, β_T^i are divided by four while μ_T^i are multiplied by four.

Table 9: Sum of the simulation results of model (7) with movement.

Measures	Location 1		Location 2		Location 3	
1	A_D^1	7.8998×10^5	A_D^2	8.2910×10^5	A_D^3	8.6320×10^5
2	A_D^1	7.6634×10^5	A_D^2	7.9359×10^5	A_D^3	7.6814×10^5
3	A_D^1	7.2907×10^5	A_D^2	7.6287×10^5	A_D^3	5.8953×10^5
1	C_D^1	1.2379×10^6	C_D^2	1.2905×10^6	C_D^3	1.3359×10^6
2	C_D^1	1.2013×10^6	C_D^2	1.2441×10^6	C_D^3	1.2033×10^6
3	C_D^1	1.1267×10^6	C_D^2	1.1978×10^6	C_D^3	8.6925×10^5
1	I_{TL}^1	9.8522×10^7	I_{TL}^2	1.8229×10^8	I_{TL}^3	4.6149×10^8
2	I_{TL}^1	6.2381×10^7	I_{TL}^2	1.1297×10^8	I_{TL}^3	2.6367×10^8
3	I_{TL}^1	3.5622×10^7	I_{TL}^2	6.3083×10^7	I_{TL}^3	1.2774×10^8
1	I_{TN}^1	1.0240×10^8	I_{TN}^2	2.7218×10^8	I_{TN}^3	5.1081×10^8
2	I_{TN}^1	6.1195×10^7	I_{TN}^2	1.6251×10^8	I_{TN}^3	2.9118×10^8
3	I_{TN}^1	2.9903×10^7	I_{TN}^2	7.9561×10^7	I_{TN}^3	1.3070×10^8
1	I_{TA}^1	5.2300×10^7	I_{TA}^2	1.0372×10^8	I_{TA}^3	2.5791×10^8
2	I_{TA}^1	3.1708×10^7	I_{TA}^2	6.2339×10^7	I_{TA}^3	1.4865×10^8
3	I_{TA}^1	1.5584×10^7	I_{TA}^2	3.0333×10^7	I_{TA}^3	6.6731×10^7

Control measures are only implemented in location 3.

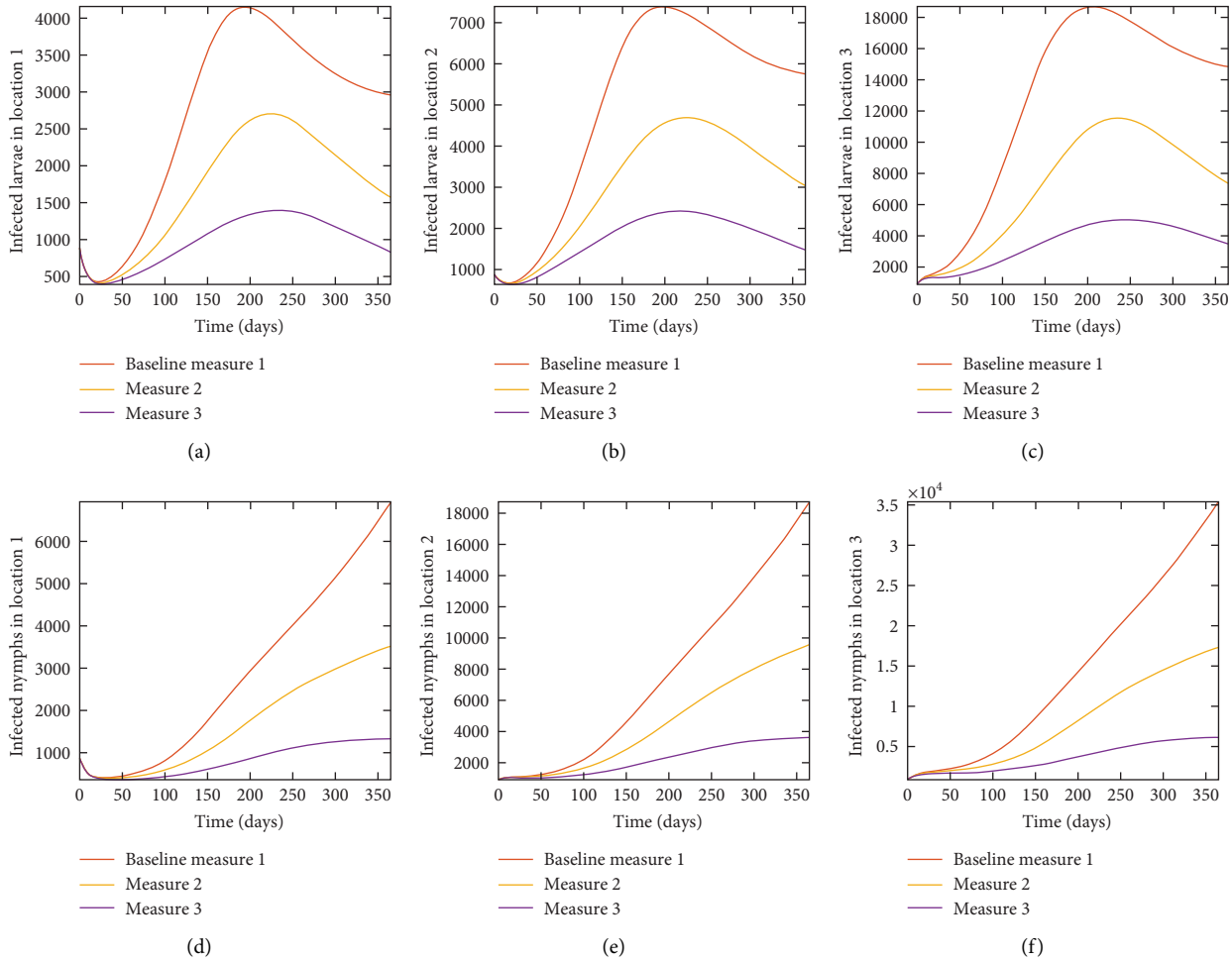

Figure 14: Continued.

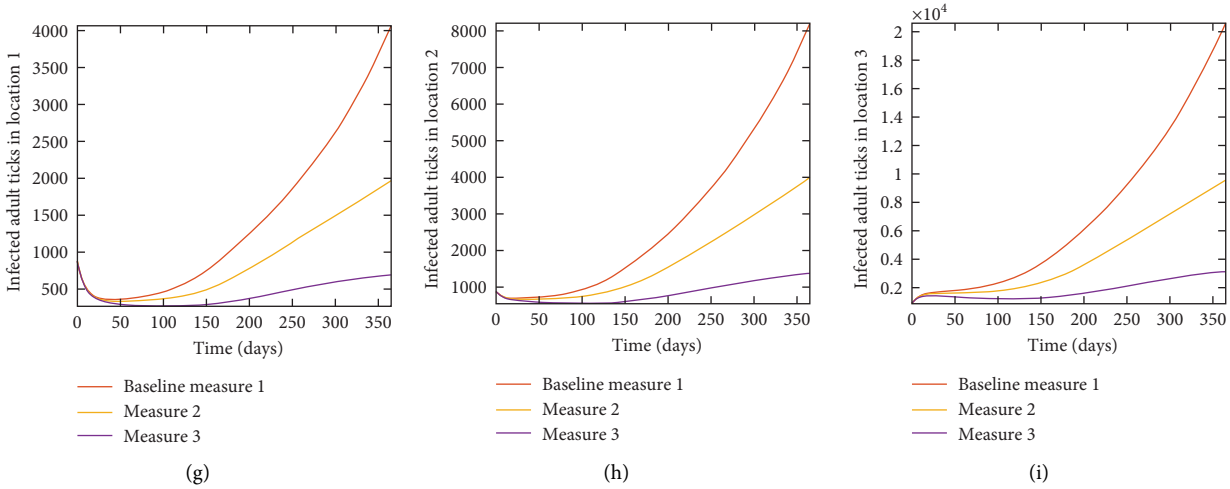

FIGURE 14: Simulation results of model (27) with movement. Control measures are implemented in location 3 only. (a–c) infected larvae; (d–f) infected nymphs; (g–i) infected adult ticks.

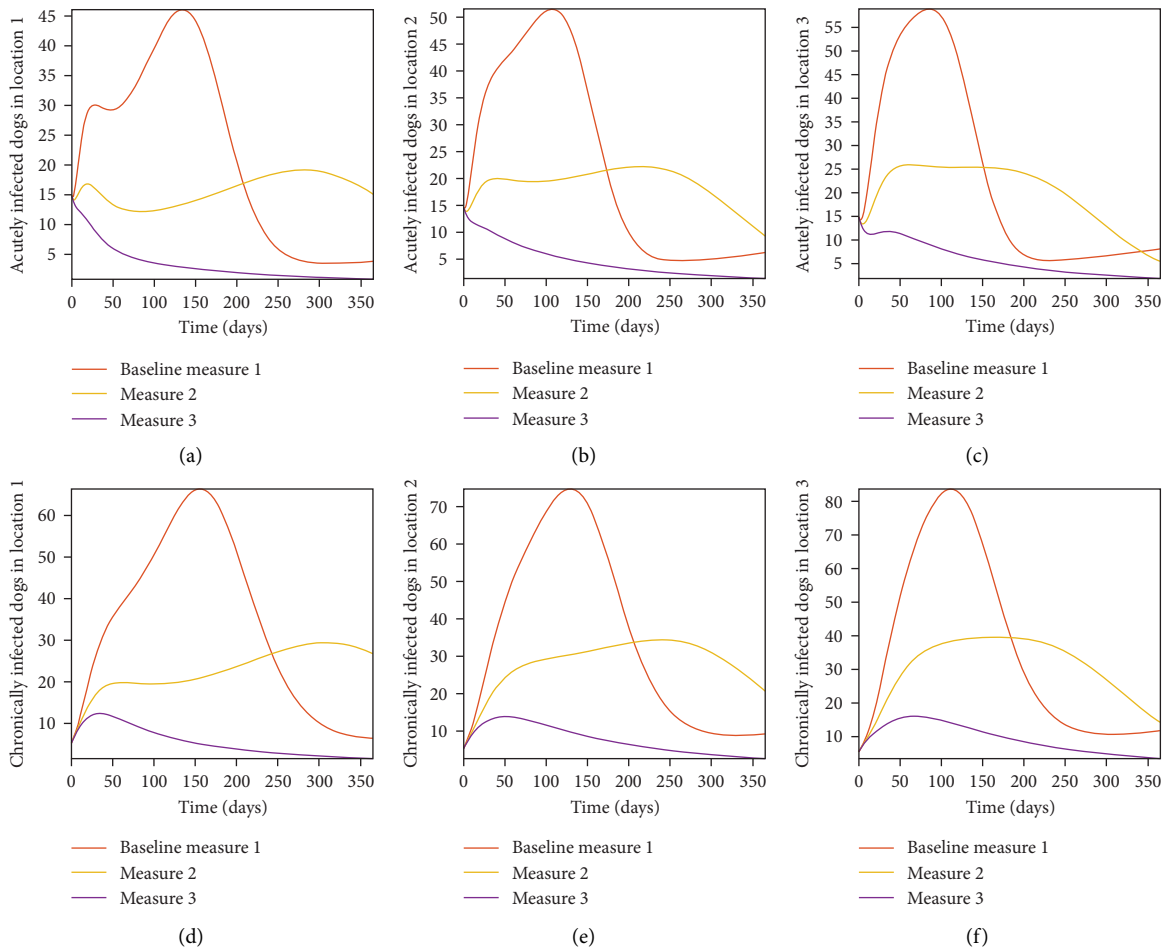

FIGURE 15: Simulation results of model (7) with movement. Control measures are implemented in all the three locations 1, 2, and 3. (a)–(c) acutely infected dogs; (d)–(f) chronically infected dogs.

Table 10: Sum of the simulation results of model (7) with movement.

Measures	Location 1		Location 2		Location 3	
1	A_D^1	8.6860×10^5	A_D^2	8.1537×10^5	A_D^3	7.6898×10^5
2	A_D^1	7.4407×10^5	A_D^2	6.5097×10^5	A_D^3	3.7349×10^5
3	A_D^1	1.9840×10^5	A_D^2	1.4660×10^5	A_D^3	9.6643×10^4
1	C_D^1	1.3523×10^6	C_D^2	1.2787×10^6	C_D^3	1.2063×10^6
2	C_D^1	1.1570×10^6	C_D^2	9.7318×10^5	C_D^3	5.5894×10^5
3	C_D^1	3.2066×10^5	C_D^2	2.4321×10^5	C_D^3	1.6682×10^5
1	I_{TL}^1	3.5822×10^8	I_{TL}^2	2.6880×10^8	I_{TL}^3	2.0342×10^8
2	I_{TL}^1	1.1852×10^8	I_{TL}^2	7.2714×10^7	I_{TL}^3	3.3064×10^7
3	I_{TL}^1	1.1374×10^7	I_{TL}^2	8.7850×10^6	I_{TL}^3	7.2365×10^6
1	I_{TN}^1	1.4126×10^8	I_{TN}^2	1.0978×10^8	I_{TN}^3	8.6427×10^7
2	I_{TN}^1	4.7045×10^7	I_{TN}^2	3.1790×10^7	I_{TN}^3	1.8848×10^7
3	I_{TN}^1	8.0034×10^6	I_{TN}^2	7.3395×10^6	I_{TN}^3	6.9439×10^6
1	I_{TA}^1	8.5854×10^7	I_{TA}^2	7.1381×10^7	I_{TA}^3	6.0548×10^7
2	I_{TA}^1	3.2641×10^7	I_{TA}^2	2.6498×10^7	I_{TA}^3	2.1308×10^7
3	I_{TA}^1	9.6459×10^6	I_{TA}^2	9.4308×10^6	I_{TA}^3	9.3019×10^6

Control measures are implemented in all three locations 1, 2, and 3.

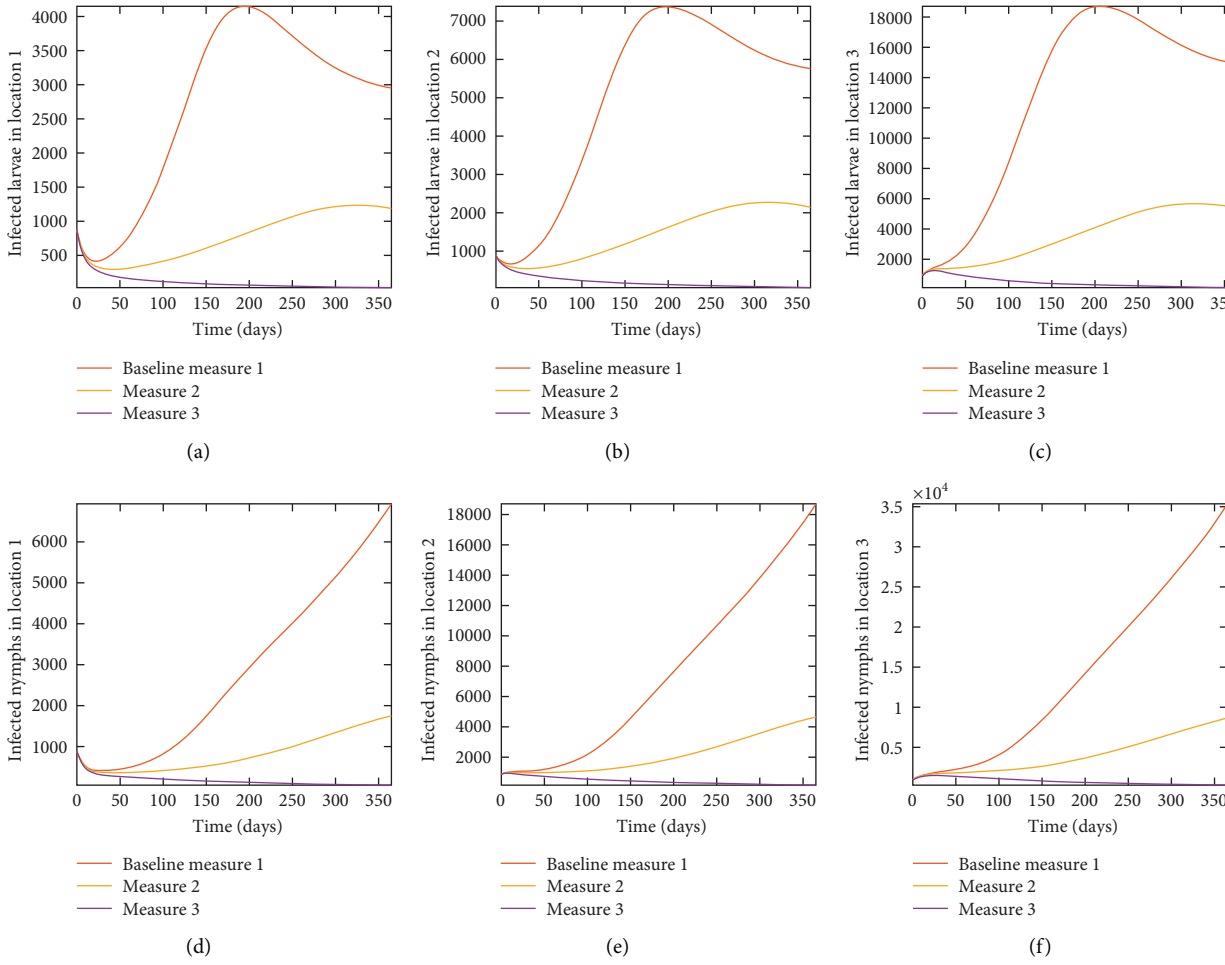

Figure 16: Continued.

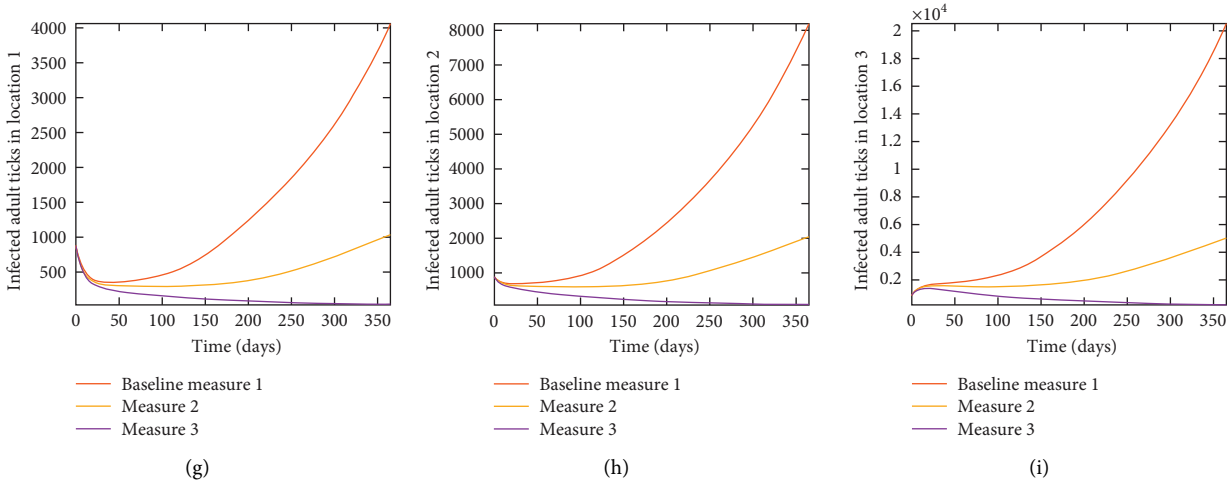

FIGURE 16: Simulation results of model (27) with movement. Control measures are implemented in all three locations 1, 2, and 3. (a–c) infected larvae; (d–f) infected nymphs; (g–i) infected adult ticks.

4.4. Connected Locations: Control in Location 1 Only. With this scenario the control measures described above are only implemented location 1. We observed in location 1, substantial reduction in population of acutely and chronically infected dogs as the control measures varies from Measures 1 through 3, see Figure 9. The effect of this measure trickles to locations 2 and 3 but the impact is minimal compare to the effect in location 1. Figure 10 shows the outcome for infected larvae, nymphs, and adult ticks in each location. Table 7 shows similar trends in the sum of the acutely and chronically infected dogs and ticks over the simulation period.

4.5. Connected Locations: Control in Location 2 Only. With this scenario the control measures described above are only implemented in location 2. Significant reduction in population of acutely and chronically infected dogs is observed in location 2 as the control measures varies from Measures 1 through 3, see Figure 11. The effect of this measure trickles to locations 1 and 3 but the impact is minimal compare to the effect in location 2. Figure 12 shows the outcome for infected larvae, nymphs, and adult ticks in each location. Similar trends can be seen in Table 8 in the values of the sum of the acutely and chronically infected dogs and ticks over the simulation period.

4.6. Connected Locations: Control in Location 3 Only. With this scenario the control measures are implemented in location 3 only. We observed in location 3, significant reduction in population of acutely and chronically infected dogs with changes in the control measures 1 through 3, see Figure 13. The effect of this measure trickles to locations 1 and 2 but the effect is minimal compare to the effect in location 3. Table 9 shows similar trends in the sum of the acutely and chronically infected dogs and ticks over the simulation period of 52 weeks. The outcome for infected larvae, nymphs, and adult ticks in each location are shown in Figure 14.

4.7. Connected Locations: Control at all Locations at the Same Time. With this scenario the three control measures described above are implemented in all three locations at the same time. We observed in all three locations significant reduction in population of acutely and chronically infected dogs using the three control measures, Measure 3 produced the most reduction see Figure 15. It is interesting to note that since similar levels of control are implemented in all three locations the effect of movement is cancelled out, as the sum of infected under this scenario is the same as the case with no movement. Similar trends are seen in Table 10 in the sum of acutely and chronically infected dogs and ticks over the simulation period. The outcome for infected larvae, nymphs, and adult ticks in each location are shown in Figure 16.

5. Discussion, Conclusion, and Recommendations

5.1. Discussion. In this paper we developed and analyzed a mathematical model (14) for the disease transmission dynamics of *Ehrlichia chaffeensis* in dogs using the natural history of infection of the disease. Features of this model include the different life stages of ticks and the different infectious stages of both dogs and ticks. The life stages of the ticks included eggs, larvae, nymphs, and adults which typically take over a two year span to complete. The infectious stages of the dogs were divided into acute and clinical/chronic. The first 2–4 weeks of infection is referred to as the acute stage. After the initial 2–4 weeks if not treated the dog will progress into a clinical/chronic stage, this stage typically leads to death [2]. *Ehrlichia chaffeensis* is a serious tick-borne infectious disease that can cause life-threatening complications. It is important to know how to prevent dogs from being infected with *Ehrlichia chaffeensis* and to be aware of the symptoms if dog becomes infected. One primary vector of *Ehrlichia chaffeensis* is the *Amblyomma americanum* ticks.

We extend the *Ehrlichia chaffeensis* model (14) by incorporating visitation and long distance migratory movements for dogs and ticks. Owners typically take their dogs on

hikes or to dog parks. It is estimated that people take their dogs on a walk about 9 times a week for around 34 minutes. This usually ends up being a two mile walk. This totals to about 370 miles a year [40]. The short dog movements were captured through the visitation parameters p_{ij}, which is the proportion of time a dog in location i spends visiting location j. Ticks long distance migratory movement may be due to ticks dropping off after feeding on either migratory birds moving north or from white-tail deer or other larger mammals [31].

Quantitative analysis of models (14) and (27) indicate that the disease-free equilibrium of these models is locally asymptotically stable when their reproduction number is less than one. Following [39], we can show that the global reproduction number of model (27) is bounded below and above by the local reproduction numbers from the patch with least and most transmission dynamics.

Next, we carried out a global sensitivity analysis using LHS/PRCC method to determine the parameter with the most influence on the response functions of sum of acutely and chronically infected $(A_D + C_D)$ and the sum of infected ticks in all life stages $(I_{TL} + I_{TN} + I_{TA})$. To implement the analysis, we used both models (14) and (27), and parameter values obtained from literature in most cases as well as assumed some where we could not find their values. The significant parameters for model (27) with movement between the locations are disease progression rate in dogs (σ_D), the rate (υ_D) dogs progress to chronic infection from acute infection, dog recovery rate (γ_D), the natural death rate of dogs (μ_D), death rate (δ_D) of acutely infected dogs, death rate of the chronically infected dogs (δ_C), birth rate of dogs (θ_D^i), the maturation rates eggs to larvae (α_E), the tick biting rate (ϕ_T^i), the dog transmission probability (β_D), the tick transmission probability (β_T^i) and death rate of ticks (μ_T^i), and the carrying capacity K^i. There parameters are also significant when we used model (14) that models transmission dynamics in a single location, see Figure 2.

Furthermore, we observed in Figures 3 that the PRCC values of parameters θ_D^i, K^i, β_D^i, β_T^i, and μ_T^i are relatively the same when there are no movement between the region. However, with movement the PRCC values for parameters θ_D^i, K^i, β_D^i, β_T^i, and μ_T^i are different, with those in location 1 having higher values than those in locations 2 and 3 since there is more movement into location 1, than 2 and 3, see Figure 4. Knowing these significant parameters is essential to the formulation of effective control strategies for combating the spread of disease. For instance, a control that aims for a 10% decrease in the transmission probability in dogs (β_D) will lead to 88% reduction in sum of acutely and chronically infected dogs and about 78% reduction in infected ticks of all life stages. Similarly a 10% decrease in the ticks' transmission probability (β_T) will lead to 71.4% reduced infection in dogs and about 83% reduced infection in ticks. Also, a 10% deduction in tick biting rate (ϕ_T) will lead to about 95% reduction in infected dogs, and about 94% reduction in infected ticks. Furthermore, a 10% increase in ticks death rate (μ_T) will result in about 72.4% reduction in infected dogs and about 83.4% decrease in ticks.

The simulation results of model (27) in Figure 5 show that locations with high infection rates like location 1 have a high number of infected dogs and ticks. This is due to the fact that the infected dogs and ticks are not moving the disease to other locations but keeping it localized in their home location. On the other hand, locations with high movement and visitation rates see an increase in infected dogs and ticks. This is due to infected dogs and ticks traveling and infecting the dogs and ticks within the location that they are visiting (in the case of dogs) and moving to (in the case of ticks). In Figures 6(a) and 6(b), we see higher number of acutely and chronically infected dogs in location 3, followed by location 2 then location 1 even though infection is higher in location 1. Similar result is observed for infected larvae, nymphs, and adult ticks in Figures 6(c), 6(d), and 6(e). These results show the impact of movement on the transmission of the disease as dogs and ticks move across locations. This result align with results in [38, 39], where the patch with the highest host movement or migration have the most infection. For instance Nguyen et al. [38] showed that deer mobility from a Lyme disease endemic county into Lyme disease free county will lead to the emergence of the disease in this second county free of the disease. Similarly, Zhang et al. [39] showed that rodent migration between patches can promote the disease spreading within all patches.

Next, we use the results from the sensitivity analysis coupled with movement between the locations to determine which control measure reduces the spread of *Ehrlichia chaffeensis* the most among dogs and ticks. Identifying these measures is crucial to decreasing the spread of *Ehrlichia chaffeensis* amongst dogs. We note that during the single location control, the effect trickles to other locations due to the effect of movement between the locations. To see the impact of this single location control trickling effect, we compare in location 2 the effect of the control measures in location 1 only where the transmission is highest to the control measures in location 3 only where movement into it is highest, but transmission is lowest, we observed that controlling in location 3 only produces the most reduction in location 2. For instance, Measure 3 for acutely infected dogs in location 2 with location 1 only control is $A_D^2 = 7.9930 \times 10^5$, while acutely infected dogs in location 2 with location 3 only control is $A_D^2 = 7.6287 \times 10^5$. Similarly for the chronically infected dogs, we have in location 2 $C_D^2 = 1.2531 \times 10^6$ with location 1 only control, while $A_D^2 = 7.6287 \times 10^5$ with location 3 only control. See Tables 5 and 7 for the other dogs and ticks variables.

5.2. Conclusion. To conclude, the goal of this study was to develop a deterministic model of ordinary differential equations to gain insight into the transmission dynamics of *Ehrlichia chaffeensis* between dogs and *Amblyomma americanum* ticks. We found that infection in dogs and ticks are localized in the absence of movement and spreads between locations with highest infection in locations with the highest rate movement. We summarize the other results as follows:

(i) The sensitivity analysis indicates that the response functions of sum of acutely and chronically infected $(A_D + C_D)$ and the sum of infected ticks at all life stages $(I_{TL} + I_{TN} + I_{TA})$ with and without movement between the locations are impacted by disease progression rate in dogs, progression rate to chronic infection in dogs, dog recovery rate, the natural death rate of dogs, disease induced death rate acutely and chronically infected dogs, birth rate of dogs, eggs maturation rates, tick biting rate, transmission probabilities in dogs and ticks, death rate of ticks, and the location carrying capacity.

(ii) In the absence of movement, locations with high infection rates have a high number of infected dogs and ticks; while locations with high movement rates see an increase in infected dogs and ticks

(iii) In the single location control, the effect of the control measures which reduces infection trickles to other locations due to the effect of movement between the locations. Furthermore, most infection reduction trickling effect is observed in location with the most movement.

5.3. Recommendations. We close by providing the following general recommendations to dog owners borne mostly out of the simulation results derived from this study which can help in the effort to effectively control the spread to the disease to their pets.

(a) Dog movement: Dog owners should limit unnecessary travel with their dogs between locations, particularly if one area has a high prevalence of *Ehrlichia chaffeensis* infection, as restricting movement can lower the risk of exposure to infected ticks. They should also be mindful of areas with high infection rates and strive to avoid them when possible. Instead, opting for safer locations with lower tick populations, such as parks, for outdoor activities with their dogs. Additionally, practicing responsible pet management by keeping dogs on a leash during walks can prevent them from wandering into tick-abundant areas with dense vegetation.

(b) Tick prevention measures: Dog owners should use tick prevention products recommended by veterinarians, such as topical treatments, collars, or oral medications, to protect their dogs from tick bites. They should regularly check their dogs for ticks after outdoor activities and promptly remove any ticks found. If dog owners must travel with their dogs to areas with different infection rates, they should closely monitor their health for any signs of illness, such as lethargy, fever, loss of appetite, or lameness. And promptly seek veterinary attention if they suspect tick-borne disease.

(c) Regular veterinary check-ups: Dog owners should schedule routine veterinary check-ups for their dogs to monitor their health status and screen for tick-borne diseases. Early detection and treatment of infections can improve outcomes and prevent the spread of disease.

These recommendations aim to help dog owners mitigate the risk of *Ehrlichia chaffeensis* and other tick-borne diseases on their pets by implementing proactive measures and promoting responsible pet care practices [41].

Appendix

A. Proof of Lemma 1

Lemma 1: Let the initial data $(0) \geq 0$, where $F(t) = (S_D(t), E_D(t), A_D(t), C_D(t), R_D(t), S_{TE}(t), S_{TL}(t), I_{TL}(t), S_{TN}(t), I_{TN}(t), S_{TA}(t), I_{TA}(t))$. Then, the solutions $F(t)$ of the *Ehrlichia chaffeensis* model (6) are non-negative for all $t > 0$. Furthermore,

$$\begin{aligned} \limsup_{t\longrightarrow\infty} N_D(t) &\leq \frac{\theta_D}{\mu_D}, \\ \limsup_{t\longrightarrow\infty} N_T(t) &\leq \frac{\sigma_E K}{\mu_T}, \end{aligned} \tag{A.1}$$

where

$$N_D(t) = S_D(t) + E_D(t) + A_D(t) + C_D(t) + R_D(t), \tag{A.2}$$

and

$$\begin{aligned} N_T(t) = {} & S_{TL}(t) + I_{TL}(t) + S_{TN}(t) \\ & + I_{TN}(t) + S_{TA}(t) + I_{TA}(t). \end{aligned} \tag{A.3}$$

Proof. Let $t_1 = \sup\{t > 0: F(t) > 0 \in [0, t]\}$. Thus, $t_1 > 0$. It follows from the first equation of the system (14), that

$$\frac{dS_D}{dt} = \theta_D - \lambda_D S_D - \mu_D S_D, \tag{A.4}$$

which can be re-written as

$$\begin{aligned} & \frac{d}{dt}\left\{S_D(t)\exp\left(\int_0^{t_1}\lambda_D(\zeta)d\zeta + \mu_D t\right)\right\} \\ & = \theta_D \exp\left(\int_0^{t_1}\lambda_D(\zeta)d\zeta + \mu_D t\right). \end{aligned} \tag{A.5}$$

Hence,

$$\begin{aligned} & S_D(t_1)\exp\left(\int_0^{t_1}\lambda_D(\zeta)d\zeta + \mu_D t_1\right) - S_D(0) \\ & = \int_0^{t_1}\theta_D \exp\left(\int_0^{p}\lambda_D(\zeta)d\zeta + \mu_D p\right)dp, \end{aligned} \tag{A.6}$$

so that,

$$S_D(t_1) = S_D(0)\exp\left[-\left(\int_0^{t_1}\lambda_D(\zeta)d\zeta + \mu_D t_1\right)\right] + \exp\left[-\left(\int_0^{t_1}\lambda_D(\zeta)d\zeta + \mu_D t_1\right)\right] \times \int_0^{t_1}\theta_D \exp\left[\left(\int_0^{p}\lambda_D(\zeta)d\zeta + \mu_D p\right)\right]dp > 0. \tag{A.7}$$

Similarly, it can be shown that $F > 0$ for all $t > 0$.

For the second part of the proof, note that $0 < S_D(0) \leq N_D(t), 0 \leq E_D(0) \leq N_D(t),\ 0 \leq A_D(0) \leq N_D(t),\ 0 < C_D(0) \leq N_D\ (t), 0 \leq R_D(0) \leq N_D(t), 0 < S_{TE}(0) \leq K, 0 < S_{TL}\ (0) \leq N_T\ (t),\ 0 \leq I_{TL}(0) \leq N_T(t),\ 0 < S_{TN}(0) \leq N_T(t),\ 0 \leq I_{TN}(0) \leq N_T(t), 0 < S_{TA}\ (0) \leq N_T(t), 0 \leq I_{TA}(0) \leq N_T(t)$.

Adding the dog and tick component of the *Ehrlichia chaffeensis* model (14) gives

$$\frac{dN_D(t)}{dt} = \theta_D - \mu_D N_D(t) - \delta_D A_D(t) - \delta_D C_D(t), \qquad \frac{dN_T}{dt} \leq \sigma_E K - \mu_T N_T. \tag{A.8}$$

We suppose that $S_E < K$, where K is the carrying capacity.

Hence,

$$\limsup_{t\longrightarrow\infty} N_D(t) \leq \frac{\theta_D}{\mu_D}, \qquad \limsup_{t\longrightarrow\infty} N_T(t) \leq \frac{\sigma_E K}{\mu_T}, \tag{A.9}$$

as required. □

B. Proof of Lemma 2

Lemma 2. The region $\Omega = \Omega_D \cup \Omega_T \subset \mathbb{R}_+^5 \times \mathbb{R}_+^7$ is positively-invariant for the model (14) with non-negative initial conditions in $\mathbb{R}_+^{12}$.

Proof. It follows from the sum of the first five equations of model (14) that

$$\frac{dN_D(t)}{dt} = \theta_D - \mu_D N_D(t) - \delta_D A_D(t) - \delta_D C_D(t), \qquad \frac{dN_D(t)}{dt} \leq \theta_A - \mu_D N_D(t). \tag{B.1}$$

Hence, $dN_D(t)/dt \leq 0$, if $N_D(0) \geq \theta_D/\mu_D$. Thus,

$$N_D(t) \leq N_D(0)e^{-\mu_D t} + \frac{\theta_D}{\mu_D}\left(1 - e^{-\mu_D t}\right). \tag{B.2}$$

In particular, if $N_D(0) \leq \theta_D/\mu_D$, then $N_D(t) \leq \theta_D/\mu_D$.

Next, the last seven equations of model (14) give the following after summing the equations representing the larvae, nymphs, and adult stages

$$\frac{dS_{TE}}{dt} = \theta_A\left(1 - \frac{S_{TE}}{K}\right)(S_{TA} + I_{TA}) - \sigma_E S_{TE} - \mu_T S_{TE}, \qquad dN_T(t) = \sigma_E E - \mu_T N_T, \tag{B.3}$$

where $\mu_T = \min\{\mu_L, \mu_N, \mu_A\}$. Since K is the carrying capacity, it follows that $S_{TE} \leq K$. Hence, equation (B.3) becomes

$$\frac{dN_T(t)}{dt} \leq \sigma_E K - \mu_T N_T. \tag{B.4}$$

Thus,

$$N_T(t) \leq \frac{\sigma_E K}{\mu_T} + \left(N_T(0) - \frac{\sigma_E K}{\mu_T}\right)e^{-\mu_T t}. \tag{B.5}$$

Furthermore, if $N_T(0) \leq \sigma_E K/\mu_T$, then $N_T(t) \leq \sigma_E K/\mu_T$.

Equations (B.2) and (B.5) imply that $N_D(t)$ and $N_T(t)$ are bounded and all solutions starting in the region Ω remain in Ω. Thus, the region is positively-invariant and hence, the region Ω attracts all solutions in $\mathbb{R}_+^{12}$. □

C. Basic Qualitative Properties of Model (27)

C.1. Positivity and Boundedness of Solutions

For the *Ehrlichia chaffeensis* transmission model (27) to be epidemiologically meaningful, it is important to prove that all its state variables are non-negative for all time. In other words, solutions of the model system (27) with non-negative initial data will remain non-negative for all time $t > 0$.

Lemma C.1. *Let the initial data* $(0) \geq 0$, *where* $F(t) = (S_D^i, E_D^i, A_D^i,\ C_D^i, R_D^i, S_{TE}^i,\ S_{TL}^i, I_{TL}^i,\ S_{TN}^i, I_{TN}^i,\ S_{TA}^i, I_{TA}^i)$. *Then, the solutions* $F(t)$ *of the Ehrlichia chaffeensis model (27) are non-negative for all* $t > 0$. *Furthermore,*

$$\limsup_{t\longrightarrow\infty} N_D(t) \leq \frac{\theta_D}{\mu_D}, \qquad \limsup_{t\longrightarrow\infty} N_T(t) \leq \frac{\sigma_E K}{\mu_T}, \tag{C.1}$$

where $N_D^i(t) = S_D^i(t) + E_D^i\ (t) + A_D^i(t) + C_D^i(t) + R_D^i\ (t), N_T^i(t) = S_{TL}^i(t) + I_{TL}^i(t) + S_{TN}^i(t) + I_{TN}^i$.

Proof. Let $t_1 = \sup\{t > 0\colon F(t) > 0 \in [0,t]\}$. Thus, $t_1 > 0$. It follows from the seventh equation of system (27), that

$$\frac{dS_{TL}^i}{dt} = \alpha_E S_{TE}^i - \frac{\beta_T^i \phi_T \left(E_D^i + A_D^i + C_D^i\right)}{N_D^i} S_{TL}^i - (\alpha_L + \mu_L) S_{TL}^i - \sum_{i \neq j}^{n} m_{ij} S_{TL}^i + \sum_{i \neq j}^{n} m_{ji} S_{TL}^j, \tag{C.2}$$

which can be re-written as

$$\frac{d}{dt}\left\{ S_{TL}^i(t) \exp\left[\left(\int_0^{t_1} \lambda_T^i(\zeta) d\zeta + k_1 t + \sum_{i=1, j \neq i}^{n} m_{ij} t \right)\right]\right\} = \left(\alpha_E S_{TE}^i + \sum_{1=1, j \neq i}^{n} m_{ji} S_{TL}^j \right) \times \exp\left[\left(\int_0^{t_1} \lambda_T^i(\zeta) d\zeta + k_1 t + \sum_{i=1, j \neq i}^{n} m_{ij} t \right)\right], \tag{C.3}$$

where $\lambda_T^i(\zeta) = (\beta_T^i \phi_T [E_D^i(\zeta) + A_D^i(\zeta) + C_D^i(\zeta)])/(N_D^i(\zeta))$, and $k_1 = \alpha_L + \mu_L$. Hence,

$$\begin{aligned} & S_{TL}^i(t_1) \exp\left[\left(\int_0^{t_1} \lambda_T^i(\zeta) d\zeta + k_1 t_1 + \sum_{i=1, j \neq i}^{n} \psi_{ij} t_1 \right)\right] - S_{TL}^i(0) \\ &= \int_0^{t_1} \left(\alpha_E S_{TE}^i(p) + \sum_{i=1, j \neq i}^{n} m_{ji} S_{TL}^j(p) \right) \\ &\quad \times \exp\left[\left(\int_0^{p} \lambda_T^i(\zeta) d\zeta + k_1 p + \sum_{i=1, j \neq i}^{n} m_{ij} p \right)\right] dp, \end{aligned} \tag{C.4}$$

so that,

$$\begin{aligned} S_{TL}^i(t_1) = S_{TL}^i(0) & \exp\left[-\left(\int_0^{t_1} \lambda_T^I(\zeta) d\zeta + k_1 t_1 + \sum_{i=i, j \neq i}^{n} m_{ij} t_1 \right)\right] \\ & + \exp\left[-\left(\int_0^{t_1} \lambda_T^i(\zeta) d\zeta + k_1 t_1 + \sum_{i=1, j \neq i}^{n} m_{ij} t_1 \right)\right] \\ & \times \int_0^{t_1} \left(\alpha_E S_{TE}^i(p) + \sum_{i=1, j \neq i}^{n} m_{ji} S_{TL}^j(p) \right) \\ & \times \exp\left[\left(\int_0^{p} \lambda_T^i(\zeta) d\zeta + k_1 t + \sum_{i=1, j \neq i}^{n} m_{ij} p \right)\right] > 0. \end{aligned} \tag{C.5}$$

Similarly, it can be shown that $F > 0$ for all $t > 0$.

For the second part of the proof, note that $0 < S_D^i(0) \leq N_D^i(t)$, $0 \leq E_D^i(0) \leq N_D^i(t)$, $0 \leq A_D^i(0) \leq N_D^i(t)$, $0 < C_D^i(0) \leq N_D^i(t), 0 \leq R_D^i(0) \leq N_D^i(t), 0 < S_{TE}^i(0) \leq K$, $0 < S_{TL}^i(0) \leq N_T^i(t)$, $0 \leq I_{TL}^i(0) \leq N_T^i(t)$, $0 < S_{TN}^i(0) \leq N_T^i(t), 0 \leq I_{TN}^i(0) \leq N_T^i(t), 0 < S_{TA}^i(0) \leq N_T^i(t), 0 \leq I_{TA}^i(0) \leq N_T^i(t)$.

Considering the dog and tick components of model (14), we have

$$\begin{aligned} \sum_{l=1}^{n} \frac{dN_D^l(t)}{dt} &= \sum_{l=1}^{n} \theta_D - \sum_{l=1}^{n} \mu_D N_D^i(t) - \sum_{l=1}^{n} \delta_D A_D^l(t) - \sum_{l=1}^{n} \delta_D C_D^l(t), \\ \sum_{l=1}^{n} \frac{dN_T^l(t)}{dt} &= \sum_{l=1}^{n} \sigma_E S_{TE}^i(t) - \sum_{l=1}^{n} \mu_T N_T^i(t) - \sum_{l=1}^{n} \left(\sum_{j=1, j \neq i}^{n} m_{ij} N_T^i(t) \right) + \sum_{l=1}^{n} \left(\sum_{j=1, j \neq i}^{n} m_{ji} N_T^j(t) \right), \end{aligned} \tag{C.6}$$

where $\mu_T = \max(\mu_L^i, \mu_N^i, \mu_A^i), i = 1, \ldots, n$. Since $S_{TE}^i(t) < K^i$, with K^i being the carrying capacity of each of region i, we have

$$\sum_{l=1}^{n} \frac{dN_D^l(t)}{dt} \leq \sum_{l=1}^{n} \theta_D - \sum_{l=1}^{n} \mu_D N_D^i(t),$$
$$\sum_{l=1}^{n} \frac{dN_T^l(t)}{dt} \leq \sum_{l=1}^{n} \sigma_E K^l - \sum_{l=1}^{n} \left(\sum_{j=1, j\neq i}^{n} m_{ij} N_T^i(t) \right) + \sum_{l=1}^{n} \left(\sum_{j=1 j\neq i}^{n} m_{ji} N_T^j(t) \right). \tag{C.7}$$

Now, summing separately the dog and tick components, gives

$$\frac{dN_D(t)}{dt} \leq \theta_D - \mu_D N_D(t),$$
$$\frac{dN_T(t)}{dt} \leq \sigma_E K - \mu_T N_T(t), \tag{C.8}$$

where with $N_D^i(t) = S_D^i(t) + E_D^i(t) + A_D^i(t) + C_D^i(t) + R_D^i(t), N_T^i(t) = S_{TL}^i(t) + I_{TL}^i(t) + S_{TN}^i(t) + I_{TN}^i$. Also,

$$-\sum_{l=1}^{n} \left(\sum_{j=1, j\neq i}^{n} m_{ij} N_T^i(t) \right) + \sum_{l=1}^{n} \left(\sum_{j=1, j\neq i}^{n} m_{ji} N_T^j(t) \right) = 0. \tag{C.9}$$

Thus, equation (C.8) leads to the following

$$\limsup_{t\longrightarrow\infty} N_D(t) \leq \frac{\theta_D}{\mu_D},$$
$$\limsup_{t\longrightarrow\infty} N_T(t) \leq \frac{\sigma_E K}{\mu_T}, \tag{C.10}$$

as required.

C.2. Invariant Regions

The *Ehrlichia chaffeensis* model (27) will be analyzed in a biologically-feasible region as follows. Consider the feasible region

$$\Omega^i = \Omega_D^i \cup \Omega_T^i \subset \mathbb{R}_+^5 \times \mathbb{R}_+^7, \tag{C.11}$$

where

$$\Omega_D^i = \left\{ \left(S_D^i(t), E_D^i(t), A_D^i(t), C_D^i(t), R_D^i(t) \right) \in \mathbb{R}_+^5 : N_D^i(t) \leq \frac{\theta_D}{\mu_D} \right\}, \tag{C.12}$$

and

$$\Omega_T^i = \left\{ \left(S_{TE}^i(t), S_{TL}^i(t), I_{TL}^i(t), S_{TN}^i(t), I_{TN}^i(t), S_{TA}^i(t), I_{TA}^i(t) \right) \in \mathbb{R}_+^7 : S_{TE}^i(t) \leq K^i, N_T^i(t) \leq \frac{\sigma_E K^i}{\mu_T} \right\}, \tag{C.13}$$

with $\mu_T = \min(\mu_L^i, \mu_N^i, \mu_A^i)$. □

Lemma C.2. *The region $\Omega_i \subset \mathbb{R}_+^{12}$ is positively-invariant for the Ehrlichia chaffeensis model (27) with non-negative initial conditions in $\mathbb{R}_+^{12}$.*

Proof. The following steps are followed to establish the positive invariance of Ω^i (i.e., solutions in Ω^i remain in Ω^i for all $t > 0$). The rate of change of the total dog and tick populations is obtained by adding separately the dog and tick component of model (27) for a particular region

$$\frac{dN_D^i(t)}{dt} = \theta_D - \mu_D N_D^i(t) - \delta_D A_D^i(t) - \delta_D C_D^i(t),$$
$$\frac{dN_T^i(t)}{dt} = \sigma_E S_{TE}^i(t) - \mu_T N_T^i(t) - \sum_{j=1, j\neq i}^{n} m_{ij} N_T^i(t) + \sum_{j=1, j\neq i}^{n} m_{ji} N_T^j(t), \tag{C.14}$$

where $\mu_T = \min(\mu_L^i, \mu_N^i, \mu_A^i)$. Since $S_{TE}^i(t) < K^i$, with K^i being the carrying capacity of each of region i, equation (C.4) reduces to

$$\begin{aligned}\frac{dN_D^i(t)}{dt} &\le \theta_D - \mu_D N_D^i(t),\\ \frac{dN_T^i(t)}{dt} &\le \sigma_E K^i - \mu_T N_T^i(t) - \sum_{j=1,j\neq i}^{n} m_{ij} N_T^i(t) + \sum_{j=1,j\neq i}^{n} m_{ji} N_T^j(t).\end{aligned} \tag{C.15}$$

From (C.15), and using a standard comparison theorem [42], we can show that

$$N_D^i(t) \le N_D^i(0) e^{-\mu_D t} + \frac{\theta_D}{\mu_D}\left(1 - e^{-\mu_D t}\right), \tag{C.16}$$

and $N_T^i(t) \le N_T^i(0) e^{-(\mu_T + \sum_{j=1,j\neq i}^{n} m_{ij} t)} + \sigma_E K^i + \sum_{j=1,j\neq i}^{n} m_{ji} N_T^j(t)\,\mu_T + \sum_{j=1,j\neq i}^{n} m_{ij}[1 - e^{-(\mu_T + \sum_{j=1,j\neq i}^{n} m_{ij})t}]$.

Furthermore, if $N_D^i(0) \le \theta_D/\mu_D$, then $N_D^i(t) \le \theta_D/\mu_D$ and $N_T^i(t) \le (\sigma_E K^i + \sum_{j=1,j\neq i}^{S} m_{ji} N^j T(t))/(\mu_T + \sum_{i=1,i\neq j}^{n} m_{ij})$, if $N_T^i(0) = (\sigma_E K^i + \sum_{j=1,j\neq i}^{n} iT_{ji} N^j T(t))/(\mu_T + \sum_{i=1,i\neq j}^{n} m_{ij})$.

Thus, the region Ω is positively-invariant. Hence, it is sufficient to consider the dynamics of the flow generated by (27) in Ω^i. In this region, the model is epidemiological and mathematically well-posed [14]. Thus, every solution of the basic model (27) with initial conditions in Ω remains in Ω for all $t > 0$. Therefore, the ω-limit sets of system (27) are contained in Ω^i. This result is summarized below. □

D. Stability of Disease-Free Equilibrium (DFE)

In the next section, the conditions for the existence and stability of the disease-free equilibrium of the model *Ehrlichia chaffeensis* (27) are stated.

The disease-free equilibrium of the *Ehrlichia chaffeensis* model (27) with movement DFE is given by

$$\overline{\mathscr{E}}_0 = \left(S_D^{i*}, E_D^{i*}, A_D^{i*}, C_D^{i*}, R_D^{i*}, S_{TE}^{i*}, S_{TL}^{i*}, I_{TL}^{i*}, S_{TN}^{i*}, I_{TN}^{i*}, S_{TA}^{i*}, I_{TA}^{i*}\right), \tag{D.1}$$

where

$$\begin{aligned}S_D^* &= \frac{\theta_D}{\mu_D},\\ S_{TE}^* &= \frac{K(\alpha_E\alpha_L\alpha_N\theta_A - g_4g_5g_7\mu_T)}{\alpha_E\alpha_L\alpha_N\theta_A},\\ S_{TL}^* &= \frac{K(\alpha_E\alpha_L\alpha_N\theta_A - g_4g_5g_7\mu_T)}{\alpha_L\alpha_N\theta_A g_5},\\ S_{TN}^* &= \frac{K(\alpha_E\alpha_L\alpha_N\theta_A - g_4g_5g_7\mu_T)}{\alpha_N\theta_A g_5g_7},\\ S_{TA}^* &= \frac{K(\alpha_E\alpha_L\alpha_N\theta_A - g_4g5g_7\mu_T)}{\theta_A\mu_T g_2g_4}.\end{aligned} \tag{D.2}$$

The stability of $\mathscr{E}_0$ can be established using the next generation matrix method on system (27). Taking $E_D, A_D, C_D, I_{TL}, I_{TN}$, and I_{TA} as the infected compartments and then using the aforementioned notation, the Jacobian $\overline{F}$ and $\overline{V}$ matrices for new infectious terms and the remaining transfer terms, respectively, are defined as.

Therefore, the reproduction is given as $\overline{\mathscr{R}}_0 = \rho(\overline{FV}^{-1})$, where

$$\begin{aligned}\overline{F} &= \begin{pmatrix} F_{11} & F_{12} & F_{13}\\ F_{21} & F_{22} & F_{23}\\ F_{31} & F_{32} & F_{33}\end{pmatrix},\\ \overline{V} &= \begin{pmatrix} V_{11} & V_{12} & V_{13}\\ V_{21} & V_{22} & V_{23}\\ V_{31} & V_{32} & V_{33}\end{pmatrix},\end{aligned} \tag{D.3}$$

with

$$F_{11}=\begin{pmatrix} 0 & 0 & 0 & p_{11}\beta_D^1\phi_T & p_{11}\beta_D^1\phi_T & p_{11}\beta_D^1\phi_T \\ 0 & 0 & 0 & 0 & 0 & 0 \\ 0 & 0 & 0 & 0 & 0 & 0 \\ \frac{\beta_T^1\phi_T S_{TL}^{1*}}{S_D^{1*}} & \frac{\beta_T^1\phi_T S_{TL}^{1*}}{S_D^{1*}} & \frac{\beta_T^1\phi_T S_{TL}^{1*}}{S_D^{1*}} & 0 & 0 & 0 \\ \frac{\beta_T^1\phi_T S_{TN}^{1*}}{S_D^{1*}} & \frac{\beta_T^1\phi_T S_{TN}^{1*}}{S_D^{1*}} & \frac{\beta_T^1\phi_T S_{TN}^{1*}}{S_D^{1*}} & 0 & 0 & 0 \\ \frac{\beta_T^1\phi_T S_{TA}^{1*}}{S_D^{1*}} & \frac{\beta_T^1\phi_T S_{TA}^{1*}}{S_D^{1*}} & \frac{\beta_T^1\phi_T S_{TA}^{1*}}{S_D^{1*}} & 0 & 0 & 0 \end{pmatrix},$$

$$V_{11}=\begin{pmatrix} g_{11} & 0 & 0 & 0 & 0 & 0 \\ -\sigma_D & g_{12} & 0 & 0 & 0 & 0 \\ 0 & -\upsilon_D & g_{13} & 0 & 0 & 0 \\ 0 & 0 & 0 & G_{15} & 0 & 0 \\ 0 & 0 & 0 & -\alpha_L & G_{16} & 0 \\ 0 & 0 & 0 & 0 & -\alpha_N & G_{17} \end{pmatrix},$$

$$F_{22}=\begin{pmatrix} 0 & 0 & 0 & p_{22}\beta_D^2\phi_T & p\beta_D^2\phi_T & p_{22}\beta_D^2\phi_T \\ 0 & 0 & 0 & 0 & 0 & 0 \\ 0 & 0 & 0 & 0 & 0 & 0 \\ \frac{\beta_T^2\phi_T S_{TL}^{2*}}{S_D^{2*}} & \frac{\beta_T^2\phi_T S_{TL}^{2*}}{S_D^{2*}} & \frac{\beta_T^2\phi_T S_{TL}^{2*}}{S_D^{2*}} & 0 & 0 & 0 \\ \frac{\beta_T^2\phi_T S_{TN}^{2*}}{S_D^{2*}} & \frac{\beta_T^2\phi_T S_{TN}^{2*}}{S_D^{2*}} & \frac{\beta_T^2\phi_T S_{TN}^{2*}}{S_D^{2*}} & 0 & 0 & 0 \\ \frac{\beta_T^2\phi_T S_{TA}^{2*}}{S_D^{2*}} & \frac{\beta_T^2\phi_T S_{TA}^{2*}}{S_D^{2*}} & \frac{\beta_T^2\phi_T S_{TA}^{2*}}{S_D^{2*}} & 0 & 0 & 0 \end{pmatrix},$$

$$V_{22} = \begin{pmatrix} g_{21} & 0 & 0 & 0 & 0 & 0 \\ -\sigma_D & g_{22} & 0 & 0 & 0 & 0 \\ 0 & -\upsilon_D & g_{23} & 0 & 0 & 0 \\ 0 & 0 & 0 & G25 & 0 & 0 \\ 0 & 0 & 0 & -\alpha_L & G_{26} & 0 \\ 0 & 0 & 0 & 0 & -\alpha_N & G_{27} \end{pmatrix},$$

$$F_{33} = \begin{pmatrix} 0 & 0 & 0 & p_{33}\beta_D^3\phi_T & p_{33}\beta_D^3\phi_T & p_{33}\beta_D^3\phi_T \\ 0 & 0 & 0 & 0 & 0 & 0 \\ 0 & 0 & 0 & 0 & 0 & 0 \\ \frac{\beta_T^3\phi_T S_{TL}^{3*}}{S_D^{3*}} & \frac{\beta_T^3\phi_T S_{TL}^{3*}}{S_D^{3*}} & \frac{\beta_T^3\phi_T S_{TL}^{3*}}{S_D^{3*}} & 0 & 0 & 0 \\ \frac{\beta_T^3\phi_T S_{TN}^{3*}}{S_D^{3*}} & \frac{\beta_T^3\phi_T S_{TN}^{3*}}{S_D^{3*}} & \frac{\beta_T^3\phi_T S_{TN}^{3*}}{S_D^{3*}} & 0 & 0 & 0 \\ \frac{\beta_T^3\phi_T S_{TA}^{3*}}{S_D^{3*}} & \frac{\beta_T^3\phi_T S_{TA}^{3*}}{S_D^{3*}} & \frac{\beta_T^3\phi_T S_{TA}^{3*}}{S_D^{3*}} & 0 & 0 & 0 \end{pmatrix},$$

$$V_{33} = \begin{pmatrix} g_{31} & 0 & 0 & 0 & 0 & 0 \\ -\sigma_D & g_{32} & 0 & 0 & 0 & 0 \\ 0 & -\upsilon_D & g_{33} & 0 & 0 & 0 \\ 0 & 0 & 0 & G_{35} & 0 & 0 \\ 0 & 0 & 0 & -\alpha_L & G_{36} & 0 \\ 0 & 0 & 0 & 0 & -\alpha_N & G_{37} \end{pmatrix},$$

$$F_{1k} = \begin{pmatrix} 0 & 0 & 0 & \frac{p_{1k}\beta_D^k\phi_T S_D^{1*}}{S_D^{k*}} & \frac{p_{1k}\beta_D^k\phi_T S_D^{1*}}{S_D^{k*}} & \frac{p_{1k}\beta_D^k\phi_T S_D^{1*}}{S_D^{k*}} \\ 0 & 0 & 0 & 0 & 0 & 0 \\ 0 & 0 & 0 & 0 & 0 & 0 \\ 0 & 0 & 0 & 0 & 0 & 0 \\ 0 & 0 & 0 & 0 & 0 & 0 \end{pmatrix},$$

$$V_{1k} = \begin{pmatrix} 0 & 0 & 0 & 0 & 0 & 0 \\ 0 & 0 & 0 & 0 & 0 & 0 \\ 0 & 0 & 0 & 0 & 0 & 0 \\ 0 & 0 & 0 & -m_{k1} & 0 & 0 \\ 0 & 0 & 0 & 0 & -m_{k1} & 0 \\ 0 & 0 & 0 & 0 & 0 & -m_{k1} \end{pmatrix},$$

$$F_{2l} = \begin{pmatrix} 0 & 0 & 0 & \frac{p_{2l}\beta_D^l \phi_T S_D^{2*}}{S_D^{l*}} & \frac{p_{2k}\beta_D^l \phi_T S_D^{2*}}{S_D^{l*}} & \frac{p_{2k}\beta_D^l \phi_T S_D^{2*}}{S_D^{l*}} \\ 0 & 0 & 0 & 0 & 0 & 0 \\ 0 & 0 & 0 & 0 & 0 & 0 \\ 0 & 0 & 0 & 0 & 0 & 0 \\ 0 & 0 & 0 & 0 & 0 & 0 \\ 0 & 0 & 0 & 0 & 0 & 0 \end{pmatrix},$$

$$V_{2l} = \begin{pmatrix} 0 & 0 & 0 & 0 & 0 & 0 \\ 0 & 0 & 0 & 0 & 0 & 0 \\ 0 & 0 & 0 & 0 & 0 & 0 \\ 0 & 0 & 0 & -m_{l2} & 0 & 0 \\ 0 & 0 & 0 & 0 & -m_{l2} & 0 \\ 0 & 0 & 0 & 0 & 0 & -m_{l2} \end{pmatrix}, \tag{D.4}$$

$$F_{3r} = \begin{pmatrix} 0 & 0 & 0 & \frac{p_{3r}\beta_D^r \phi_T S_D^{3*}}{S_D^{r*}} & \frac{p_{3r}\beta_D^r \phi_T S_D^{3*}}{S_D^{r*}} & \frac{p_{3r}\beta_D^r \phi_T S_D^{3*}}{S_D^{r*}} \\ 0 & 0 & 0 & 0 & 0 & 0 \\ 0 & 0 & 0 & 0 & 0 & 0 \\ 0 & 0 & 0 & 0 & 0 & 0 \\ 0 & 0 & 0 & 0 & 0 & 0 \\ 0 & 0 & 0 & 0 & 0 & 0 \end{pmatrix},$$

$$V_{3r} = \begin{pmatrix} 0 & 0 & 0 & 0 & 0 & 0 \\ 0 & 0 & 0 & 0 & 0 & 0 \\ 0 & 0 & 0 & 0 & 0 & 0 \\ 0 & 0 & 0 & -m_{r3} & 0 & 0 \\ 0 & 0 & 0 & 0 & -m_{r3} & 0 \\ 0 & 0 & 0 & 0 & 0 & -m_{r3} \end{pmatrix},$$

and $k = 2, 3, l = 1, 3, r = 1, 2, g_{11} = \sigma_D + \mu_D, g_{12} = \upsilon_D + \gamma_D + \mu_D + \delta_D$, $g_{13} = \mu_D + \delta_C, g_{14} = \alpha_E + \mu_E, g_{15} = \alpha_L + \mu_T^1, g_{15} = \alpha_L + \mu_T^1, g_{16} = \alpha_N + \mu_T^1, g_{16} = \alpha_N + \mu_T^1, g_{21} = \sigma_D + \mu_D$, $g_{22} = \upsilon_D + \gamma_D + \mu_D + \delta_D, g_{23} = \mu_D + \delta_C, g_{24} = \alpha_E + \mu_E, g_{25} = \alpha_L + \mu_T^2, g_{25} = \alpha_L + \mu_T^2, g_{26} = \alpha_N + \mu_T^2, g_{26} = \alpha_N + \mu_T^2, g_{31} = (\sigma_D + \mu_D), g_{32} = \upsilon_D + \gamma_D + \mu_D + \delta_D, g_{33} = \mu_D + \delta_C$, $g_{34} = \alpha_E + \mu_E, g_{35} = \alpha_L + \mu_T^3, g_{35} = \alpha_L + \mu_T^3, g_{36} = \alpha_N + \mu_T^3, g_{36} = \alpha_N + \mu_T^3, G_{15} = g_{15} + (m_{12} + m_{13}), G_{16} = g_{16} + (m_{12} + m_{13}), G_{17} = \mu_T^1 + (m_{12} + m_{13}), \quad G_{25} = g_{25} + (m_{21} + m_{23}), G_{26} = g_{26} + (m_{21} + m_{23}), \quad G_{27} = \mu_T^2 + (m_{21} + m_{23}), \quad G_{35} = g_{35} + (m_{31} + m_{32}), G_{36} = g_{36} + (m_{31} + m_{32}), G_{37} = \mu_T^3 + (m_{31} + m_{32})$.

The following result is established using Theorem 2 in [12].

Lemma D.1. *The DFE of the Ehrlichia chaffeensis model (27) with movement, given by* $\overline{\mathscr{E}}_0$*, is locally asymptotically stable (LAS) if* $\overline{\mathscr{R}}_0 < 1$*, and unstable if* $\overline{\mathscr{R}}_0 > 1$.

The basic reproduction number ($\overline{\mathscr{R}}_0$) measures the average number of new infections generated by a single infected individual (tick or dog) in a completely susceptible population [6, 16, 20, 39]. Thus, Lemma D.1 implies that malaria can be eliminated from the human population (when $\overline{\mathscr{R}}_0 < 1$) if the initial sizes of the subpopulations are in the basin of attraction of the DFE, $\overline{\mathscr{E}}_0$.

Data Availability

No dataset was used in this study.

Conflicts of Interest

The authors declare that there are no conflicts of interest regarding the publication of this paper.

Acknowledgments

This project was supported by the National Science Foundation under the EPSCOR Track 2 Grant no. 1920946.

References

[1] J. Sellman, "Vietnam war dogs and an unknown new disease," 2023.

[2] K. Williams, R. Llera, and E. Ward, "Ehrlichiosis in dogs," 2022, https://vcahospitals.com/know-your-pet/ehrlichiosis-in-dogs.

[3] Center for Disease Prevention and Control (Cdc), *Transmission and Epidemeology*.

[4] Indiana Department of Health, *Amblyomma americanum*.

[5] University of Rhode Island, "Lone star tick," 2022, https://web.uri.edu/tickencounter/species/lone-star-tick/.

[6] Center for Disease Prevention and Control (Cdc), *Ehrlichiosis in Dogs: Fast Facts for Veterinarians*.

[7] A. Sainz, X. Roura, G. Miró et al., *Guideline for Veterinary Practitioners on Canine Ehrlichiosis and Anaplasmosis in Europe*.

[8] F. Agusto and J. Drum, "Modeling the effects of Ehrlichia chaffeensis and movement on dogs," *bioRxiv*, pp. 2023–2111, 2023.

[9] F. B. Agusto, R. Djidjou-Demasse, and O. Seydi, "Mathematical model of Ehrlichia chaffeensis transmission dynamics in dogs," *Journal of Biological Dynamics*, vol. 17, no. 1, p. 2287082, Article ID 2287082, 2023.

[10] L. Leonardi, "Identify ehrlichiosis symptoms at all 3 stages of the disease learn what signs to watch out for," 2022.

[11] Science Direct, "Amblyomma americanum".

[12] P. van den Driessche and J. Watmough, "Reproduction numbers and sub-threshold endemic equilibria for compartmental models of disease transmission," *Mathematical Biosciences*, vol. 180, no. 1-2, pp. 29–48, 2002.

[13] O. Diekmann, J. A. P. Heesterbeek, and J. A. P. Metz, "On the definition and the computation of the basic reproduction ratio R 0 in models for infectious diseases in heterogeneous populations_{0} in models for infectious diseases in heterogeneous populations," *Journal of Mathematical Biology*, vol. 28, no. 4, pp. 503–522, 1990.

[14] H. W. Hethcote, "The mathematics of infectious diseases," *SIAM Review*, vol. 42, no. 4, pp. 599–653, 2000.

[15] North Shore Animal League, "Prevent a litter-spay and neuter your pets," 2022.

[16] Mar Vista Animal Medical Center, *Ehrlichia infection (canine)*, 2020.

[17] C. Wheeler, "The life cycle of a tick," 2022, https://study.com/learn/lesson/tick-life-cycle-reproduction-eggs.html.

[18] A. Ludwig, H. S. Ginsberg, G. J. Hickling, and N. H. Ogden, "A dynamic population model to investigate effects of climate and Climate-independent factors on the lifecycle of*Amblyomma americanum*(Acari: Ixodidae)," *Journal of Medical Entomology*, vol. 53, no. 1, pp. 99–115, 2015.

[19] A. Burke, *How Long Do Dogs Live?*

[20] S. Harrus, P. H. Kass, E. Klement, and T. Waner, "Canine monocytic ehrlichiosis: a retrospective study of 100 cases, and an epidemiological investigation of prognostic indicators for the disease," *The Veterinary Record*, vol. 141, no. 14, pp. 360–363, 1997.

[21] M. Small and R. E. Brennan, "Detection of rickettsia amblyommatis and Ehrlichia chaffeensis in amblyomma americanum inhabiting two urban parks in Oklahoma," 2022.

[22] R. W. Atherton, R. B. Schainker, and E. R. Ducot, "On the statistical sensitivity analysis of models for chemical kinetics," *AIChE Journal*, vol. 21, no. 3, pp. 441–448, 1975.

[23] N. Chitnis, J. M. Hyman, and J. M. Cushing, "Determining important parameters in the spread of malaria through the sensitivity analysis of a mathematical model," *Bulletin of Mathematical Biology*, vol. 70, no. 5, pp. 1272–1296, 2008.

[24] D. M. Hamby, "A review of techniques for parameter sensitivity analysis of environmental models," *Environmental Monitoring and Assessment*, vol. 32, no. 2, pp. 135–154, 1994.

[25] S. M. Blower and H. I. Dowlatabadi, "Sensitivity and uncertainty analysis of complex models of disease transmission: an hiv model, as an example," *International Statistical Review/Revue Internationale de Statistique*, vol. 62, no. 2, pp. 229–243, 1994.

[26] S. Marino, I. B. Hogue, C. J. Ray, and D. E. Kirschner, "A methodology for performing global uncertainty and sensitivity analysis in systems biology," *Journal of Theoretical Biology*, vol. 254, no. 1, pp. 178–196, 2008.

[27] M. D. McKay, R. J. Beckman, and W. J. Conover, "A comparison of three methods for selecting values of input variables in the analysis of output from a computer code," *Technometrics*, vol. 42, no. 1, pp. 55–61, 2000.

[28] M. A. Sanchez and S. M. Blower, "Uncertainty and sensitivity analysis of the basic reproductive rate: tuberculosis as an

example," *American Journal of Epidemiology*, vol. 145, no. 12, pp. 1127–1137, 1997.
[29] F. Agusto, A. Goldberg, O. Ortega et al., "How do interventions impact malaria dynamics between neighboring countries? a case study with Botswana and Zimbabwe," *Association for Women in Mathematics Series*, pp. 83–109, 2021.
[30] C. A. Torre, *Deterministic and Stochastic Metapopulation Models for Dengue Fever*, Arizona State University, 2009.
[31] J. M Heffernan, Y. Lou, and J. Wu, "Range expansion of ixodes scapularis ticks and of borrelia burgdorferi by migratory birds," *Discrete & Continuous Dynamical Systems-B*, vol. 19, no. 10, pp. 3147–3167, 2014.
[32] C. Cosner, J. C. Beier, R. S. Cantrell et al., "The effects of human movement on the persistence of vector-borne diseases," *Journal of Theoretical Biology*, vol. 258, no. 4, pp. 550–560, 2009.
[33] S. Ruan, W. Wang, and S. A Levin, "The effect of global travel on the spread of sars," *Mathematical Biosciences and Engineering*, vol. 3, no. 1, pp. 205–218, 2006.
[34] F. B. Agusto, "Malaria drug resistance: the impact of human movement and spatial heterogeneity," *Bulletin of Mathematical Biology*, vol. 76, no. 7, pp. 1607–1641, 2014.
[35] F. B. Agusto and S. Kim, "Impact of mobility on methicillin-resistant staphylococcus aureus among injection drug users," *Antibiotics*, vol. 8, no. 2, p. 81, 2019.
[36] J. Arino, J. R. Davis, D. Hartley, R. Jordan, J. M. Miller, and P. van den Driessche, "A multi-species epidemic model with spatial dynamics," *Mathematical Medicine and Biology: A Journal of the IMA*, vol. 22, no. 2, pp. 129–142, 2005.
[37] M. Maliyoni, H. D. Gaff, K. S. Govinder, and F. Chirove, "Multipatch stochastic epidemic model for the dynamics of a tick-borne disease," *Frontiers in Applied Mathematics and Statistics*, vol. 9, Article ID 1122410, 2023.
[38] A. Nguyen, J. Mahaffy, and N. K. Vaidya, "Modeling transmission dynamics of lyme disease: multiple vectors, seasonality, and vector mobility," *Infectious Disease Modelling*, vol. 4, pp. 28–43, 2019.
[39] X. Zhang, B. Sun, and Y. Lou, "Dynamics of a periodic tick-borne disease model with co-feeding and multiple patches," *Journal of Mathematical Biology*, vol. 82, no. 4, pp. 17–27, 2021.
[40] S. Coren, "How many people don't walk their dogs?"
[41] R. M. Anderson and R. May, *Infectious Diseases of Humans*, Oxford University Press, New York, 1991.
[42] V. Lakshmikantham, S. Leela, and A. A. Martynyuk, *Stability Analysis of Nonlinear Systems*, Springer, 1989.